Differentiation signals from glia are fine-tuned to set neuronal numbers during development

Anadika R. Prasad[1], Inês Lago-Baldaia[1], Matthew P. Bostock[1], Zaynab Housseini[1] and Vilaiwan M. Fernandes[1]*.

[1]Department of Cell and Developmental Biology, University College London, Gower Street, London, WC1E 6DE.

*Corresponding author; vilaiwan.fernandes@ucl.ac.uk

Summary: Neural circuit formation and function require that diverse neurons are specified in appropriate numbers. Known strategies for controlling neuronal numbers involve regulating either cell proliferation or survival. We used the *Drosophila* visual system to probe how neuronal numbers are set. Photoreceptors from the eye-disc induce their target field, the lamina, such that for every unit eye there is a corresponding lamina unit (column). Although each column initially contains ~6 post-mitotic lamina precursors, only 5 differentiate into neurons, called L1-L5; the 'extra' precursor, which is invariantly positioned above the L5 neuron in each column, undergoes apoptosis. By forcing neuronal differentiation in the lamina, we uncovered that though fated to die, the 'extra' precursor is specified as an L5. Therefore, two precursors are specified as L5s but only one differentiates during normal development. We showed that a glial population called the outer chiasm giant glia (xg^O), which resides below the lamina, secretes multiple ligands to induce L5 differentiation in response to EGF from photoreceptors. The row of precursors nearest to xg^O differentiate into L5s and, in turn, antagonise differentiation signalling to prevent the 'extra' precursors from differentiating, resulting in their death. Thus, an intricate interplay of glial signals and feedback from differentiating neurons defines an invariant and stereotyped pattern of neuronal differentiation and programmed cell death to ensure that lamina columns each contain exactly one L5 neuron. In sum, neuronal numbers can be set by inducing differentiation of a subset of neurons from a larger pool of specified progenitors.

Keywords: Neuronal numbers, Glia, *Drosophila* visual system, Neuronal differentiation, Programmed cell death

Introduction

Many sensory systems consist of repeated circuit units that map stimuli from the outside world onto sequential processing layers[1]. It is critical that both absolute and relative neuronal numbers are carefully controlled for these circuits to assemble with topographic correspondence across processing layers. Neuronal numbers can be set by controlling how many progeny a neural stem cell produces, or by regulating how many neural progeny survive[2,3]. To investigate other developmental strategies that set neuronal numbers, we used the highly ordered and repetitive *Drosophila melanogaster* visual system. Like vertebrate visual systems, the fly visual system is organized retinotopically into repeated modular circuits that process sensory input from unique points in space spanning the entire visual field[4,5].

Retinotopy between the compound eye and the lamina is built during development. Photoreceptors are born progressively in the eye imaginal disc as a wave of differentiation sweeps across the tissue from posterior to anterior. Newly born photoreceptors express Hedgehog (Hh), which promotes further wave propagation[6]. They also express the Epidermal Growth Factor (EGF), Spitz (Spi), which recruits additional photoreceptors into developing ommatidia[6]. As photoreceptors are born, their axons project into the optic lobe and induce the lamina, such that there is a corresponding lamina unit for every ommatidium (Fig. 1A)[4]. Each unit is composed of five interneurons (L1-L5; named for the medulla layers they project to) and multiple glial subtypes[4,7].

Lamina induction is a multi-step process triggered by photoreceptor-derived signals. Photoreceptor-derived Hh converts neuroepithelial cells into lamina precursor cells (LPCs), promotes their terminal divisions and orchestrates lamina column assembly, *i.e.* the stacked association of ~6 post-mitotic LPCs with photoreceptor axon bundles (Fig. 1A,B)[8–11]. Once assembled into columns, LPCs differentiate into neurons following an invariant spatio-temporal pattern whereby the most proximal (bottom) and most distal (top) cells differentiate first into L5 and L2, respectively; differentiation then proceeds in a distal-to-proximal (top-to-bottom) sequence, L3 forming next, followed by L1, then L4[12–14]. The sixth LPC, located between L4 and L5, does not differentiate but instead is fated to die by apoptosis and is later cleared (Fig. 1A)[15]. Previously we showed that a population of glia called wrapping glia, which ensheathes photoreceptor axons, induces neuronal differentiation of L1-L4 neurons via Insulin/ Insulin-like growth factor signalling in response to EGF from photoreceptors[14]. Intriguingly, L1-L4 neuronal

differentiation could be disrupted by manipulating wrapping glia without affecting L5 differentiation[14]. Indeed, the mechanisms that drive L5 differentiation are not known. Importantly, we do not understand how exactly 5 neuron types differentiate from 6 apparently equal LPCs; in other words, how are lamina neuronal numbers set?

Here, we set out to determine the mechanisms that induce L5 differentiation. We found that the 'extra' LPCs normally eliminated by apoptosis are specified with L5, but not L1-L4, identity. Further, we identified that a population of glia called the outer chiasm giant glia (xg^O), located proximal to the lamina plexus, induces L5 differentiation in response to photoreceptor-EGF. We showed that xg^O secrete multiple signals, including the EGF Spi and a type IV collagen, Collagen type IV alpha 1 (Col4a1) to induce neuronal differentiation and promote survival through Mitogen-Activated Protein Kinase (MAPK) activity. Since the most proximal row of LPCs are in closest proximity to the xg^O, they receive xg^O cues first and differentiate into L5s. Finally, we showed that these newly induced L5s secrete high levels of Argos (Aos), an antagonist of Spi[16], which limits MAPK activity in the 'extra' LPCs thus preventing their differentiation. Altogether, our results indicate that the pattern of neuronal differentiation and programmed cell death in the lamina are determined by the architecture of the developing tissue together with feedback from newly differentiating neurons.

Results

The 'extra' lamina precursor cells are specified as L5s

To probe how only five lamina neurons are invariantly produced from a pool of six seemingly equivalent precursors, we began by focusing on the 'extra' LPCs, which are located distal to L5s[9]. To confirm that these cells do indeed undergo apoptosis in normal development, we used an antibody against the cleaved form of Death Caspase-1 (Dcp-1), an effector caspase, to detect apoptotic cells[17]. In wild-type animals, we detected Dcp-1 positive apoptotic cells in the lamina immediately distal to L5 neurons starting from column 5.15 ± 0.25 (Standard Error of the Mean; N=13; Fig. 1C). Note that for these and later analyses we considered the youngest column located adjacent to the lamina furrow to be the first column, with column number (and age) increasing towards the posterior side of the furrow (right side in Fig. 1A). Next, we examined the fate of these cells when apoptosis was blocked in animals mutant for *Death regulator Nedd2-like caspase (Dronc)*, an initiator caspase essential for caspase-dependent cell death[18]. Cleaved Dcp-1

was absent in homozygous *Dronc*^{I24} animals confirming that apoptosis was blocked (N=26; Fig. 1E). Indeed, we detected cells that were positive for the lamina marker Dachshund (Dac) but negative for the pan-neuronal marker Elav between L1-L4 and L5 neurons past column 5, which were never observed in controls (Fig. 1E compared to 1C; N=13). These cells did not express lamina neuron subtype markers Sloppy paired 2 (Slp2) or Brain-specific homeobox (Bsh), which L5s co-express and which individually label L1-L3s and L4s, respectively (Fig. 1D,F)[13,14,19]. Thus, although the 'extra' LPCs were retained when apoptosis was blocked, they did not differentiate into neurons.

Since preventing apoptosis of the 'extra' LPCs did not reveal their neuronal potential, we sought to force their differentiation. Previously, we showed that MAPK signalling is necessary and sufficient to drive L1-L4 neuronal differentiation[14]. High levels of double-phosphorylated MAPK (dpMAPK), indicative of pathway activity, preceded neuronal differentiation (assessed by Elav expression), not just for L1-L4s, but also for L5s (Fig. 1G; N=7), suggesting that MAPK signalling is involved in differentiation for all neuronal types. Therefore, we hyperactivated the pathway by using a lamina-specific Gal4 to drive an activated form of MAPK (MAPK^{ACT}) or of a transcriptional effector of the pathway, Pointed P1 (PntP1). Importantly, we combined this Gal4 with a temperature sensitive form of Gal80, Gal80^{ts}, to restrict expression during development; this driver is referred to as *Lamina*^{ts} henceforth (Fig. S1C,D and Fig. 1H,I). As reported previously, hyperactivating MAPK signalling in the lamina led to premature neuronal differentiation: instead of sequential differentiation of L1-L4, seen as a triangular front, most lamina columns differentiated simultaneously (Fig. 1H, N=17, Fig. S1A,C, N=10)[14]. We observed no LPCs that remained undifferentiated (Dac^{+} and Elav^{-}) past lamina column 5, including the row of cells just distal to L5s (Fig. 1H, S1A,C). Interestingly, we also observed a concomitant decrease in cleaved Dcp-1 positive cells (Fig. 1H, J), suggesting that forcing the 'extra' LPCs to differentiate blocked their death.

We next asked which lamina neuron subtype the 'extra' LPCs could give rise to when induced to differentiate. Using Slp2 and Bsh to distinguish between lamina neurons, we often observed two rows of cells co-expressing Slp2 and Bsh in the proximal lamina (Fig. 1I, S1B,D), indicating the presence of ectopic L5s. However, the presence of ectopic cells could be due to premature differentiation, rather than ectopic induction of a particular cell type. In control animals, columns are fully differentiated (Elav+) from column 7 onwards (Fig. S1E). Therefore,

to distinguish between premature and ectopic differentiation, we quantified the number of lamina neuron types (L1-L3, L4 and L5) per column from column 7 onwards. While there was no significant difference between the average number of L1-L3s or L4s per column, the average number of L5s/column was ~1.4-fold higher in laminas in which differentiation was ectopically induced compared with controls (Figs. 1K,L). Thus, hyperactivating MAPK signalling in the lamina drives ectopic differentiation of L5 neurons. Importantly, ectopic L5s were only observed in the proximal but never in the distal lamina (Fig. 1I, N=18/18; Fig. S1D, N=9/9). Taken together, the absence of cell death in the row distal to L5s and the presence of ectopic L5s in this row indicate that hyperactivating MAPK signalling induces the 'extra' LPCs to differentiate into L5s. Thus, LPCs are not equivalent; instead, they are patterned with fixed neuronal identities along the distal to proximal axis, such that the two most proximal rows of LPCs are specified as L5s and differentiate accordingly when induced.

Outer chiasm giant glia (xg^O) induce L5 neuronal differentiation in response to EGF from photoreceptors

Although the two most proximal rows of LPCs are specified as L5s, in normal development only one row is fated to differentiate into L5 neurons, while the other is fated to die. This led us to ask how neuronal differentiation and apoptosis are regulated to produce exactly one L5 neuron per column. Since we showed previously that wrapping glia induce L1-L4 neuronal differentiation in response to EGF from photoreceptors, but that L5 differentiation proceeded normally in these conditions[14], we speculated that another glial population may be involved in inducing L5 differentiation in response to EGF from photoreceptors. To test this hypothesis, we blocked EGFR signalling in all glia using a pan-glial driver. This led to a complete block in lamina neuron differentiation as seen by the absence of any Elav positive cells, though LPCs (Dac+ cells) still formed and assembled into columns (Fig. 2A,B). Thus, EGFR activity in a glial population other than the wrapping glia is required for L5 neuronal differentiation.

Many glial types infiltrate the lamina (Fig. S2A)[20,21]. Therefore, we performed a screen using glia subtype-specific Gal4s to block EGFR signalling and evaluated the presence of L5s using Elav expression (Fig. S2B-M; summarised in Table S1). Blocking EGFR signalling in the outer chiasm giant glia (xg^O) led to a dramatic reduction in the number of L5s (Fig. 2C,D, S2N; See Supplementary text). The xg^O are located below the lamina plexus, often with just one or two

cells spanning the entire width of the lamina. While the xg^O extend fine processes towards the lamina, they do not appear to contact LPCs or L5 neurons (Fig. S2O). Moreover, blocking EGFR signalling in the xg^O did not affect xg^O numbers or morphology (Fig. 2C,D, S2O-R). Since our screen used Elav and proximal location in the lamina to assess for the presence of L5s, we sought to confirm whether L5s were indeed affected when EGFR activity was blocked in xg^O. We used antibodies against Bsh and Slp2 as before, together with Svp, which marks L1s, to identify and count lamina neurons. We found that the numbers of L5 neurons were specifically decreased, while numbers of all the other neuron types were unaffected (Fig. 2E-G; $P^{L5}<0.0001$, Mann-Whitney U-test). To test whether the absence of L5s simply reflected a developmental delay, we examined adult optic lobes using a different L5 neuronal marker, POU domain motif 3 (Pdm3)[13]. Similar to our results in the larval lamina, L5s were mostly absent in the adult lamina when EGFR was blocked in xg^O compared with controls (Fig. S2S,T; $N^{exp}=10$; $N^{ctrl}=11$), indicating that the loss of L5s observed in larvae is not due to delayed induction.

The loss of L5 neurons when EGFR was blocked in xg^O could be explained either by a defect in neuronal differentiation, or by an earlier defect in LPC formation or recruitment to columns. To distinguish between these possibilities, we counted the number of LPCs per column when EGFR signalling was blocked in xg^O compared to controls (Fig. 2H). In columns 1-4, there were no differences in the number of LPCs, indicating that LPC formation and column assembly occurred normally. Thus, although LPCs formed and assembled into columns normally, L5s failed to differentiate; supporting the hypothesis that in response to EGFR activity xg^O induce proximal LPC neuronal differentiation into L5s. Importantly, the number of LPCs began to decrease in older columns (column 5 onwards) when EGFR signalling was blocked in xg^O (Fig. 2H). This observation suggested that undifferentiated LPCs in the proximal lamina were eliminated by apoptosis, similar to the 'extra' LPCs in controls. Consistently, we observed Dcp-1 positive cells in the most proximal row of the lamina beginning on average in column 5.93 ± 0.18 (N=19; Fig. 2I,J). Altogether these results show that EGFR activity in xg^O induces the differentiation of L5 neurons, and that proximal LPCs which fail to receive appropriate cues from xg^O die by apoptosis.

Next, we sought to determine which cells were inducing/what was the source of EGFR activity in xg^O. Since EGFR activity in wrapping glia is triggered by EGF from photoreceptors[14], we tested whether photoreceptor-EGF could also contribute to activating EGFR in xg^O. We took

advantage of a mutant for *rhomboid 3 (rho3)* in which photoreceptors are specified but cannot secrete Spi from their axons[22], resulting in failure of L1-L4 neurons to differentiate (Fig. 2K; N=9)[14,22]. In addition to disrupted L1-L4 neuronal differentiation, we previously showed that only a few L5 neurons differentiated in *rho3* animals (Fig. 2K; N=9)[14]. To test whether xg^O induce L5 neuronal differentiation in response to photoreceptor-EGF, we restored expression of wild-type Rho3 only in photoreceptors in *rho3* mutant animals using a photoreceptor-specific driver (GMR-Gal4). Rho3 function in photoreceptors was sufficient to fully rescue not only L1-L4 neuronal differentiation, as previously reported, but also L5 neuronal differentiation (Fig. 2L; N=8). Thus, similar to wrapping glia for L1-L4s, xg^O respond to EGF from photoreceptors to induce differentiation of proximal LPCs into L5 neurons.

Outer chiasm giant glia secrete multiple ligands to induce MAPK-dependent neuronal differentiation of L5s.

We next asked what signals the xg^O secrete to induce L5 differentiation. Since autonomously hyperactivating MAPK signalling in LPCs was sufficient to drive ectopic L5 neuronal differentiation (Fig. 1H, I, S1C,D), the signals inducing differentiation likely act upstream of the MAPK signal transduction cascade. We first confirmed that MAPK signalling is necessary for L5 neuronal differentiation, and moreover showed that reducing MAPK activity results in death of LPCs (See Supplementary text and Figs. S3A-D). Given this requirement, we reasoned that the differentiation signals from xg^O must lead to activation of MAPK signalling in proximal LPCs, likely through a Receptor Tyrosine Kinase (RTK). Indeed, blocking EGFR signalling in xg^O resulted in decreased dpMAPK levels specifically in the proximal lamina (Fig. S3E compared with 1G). The *Drosophila* genome encodes 22 ligands which activate 10 RTKs upstream of MAPK signalling[23]. To identify the signal(s) secreted by xg^O, we overexpressed these ligands and screened for their ability to rescue the loss of L5s caused by blocking EGFR activity in the xg^O. To validate this approach, we tested whether autonomously restoring transcriptional activity downstream of MAPK in xg^O while blocking EGFR activity could rescue L5 differentiation. While blocking EGFR in xg^O resulted in laminas containing 7.3% ±1.6 of the control number of L5s, co-expressing PntP1 with $EGFR^{DN}$ in xg^O rescued L5 numbers to 24.7% ±2.9 of control laminas ($P<0.0001$ compared to EGFR DN alone; Fig. S3F). We then screened 18 ligands based on available reagents (Fig. S3F). Four ligands resulted in statistically significant

rescues of L5 numbers when overexpressed in xg^O (Fig. S3F). To eliminate false positive hits, we examined enhancer trap lines and published reports to determine whether these ligands are expressed in xg^O under physiological conditions (See Supplementary text and Fig. S3G-J). This enabled us to narrow down our hits to two ligands: the EGF Spi and Col4a1, a type IV collagen, which both rescued L5 differentiation resulting in laminas with 17.4% ±1.9 and 19.7% ±2.2 of the control number of L5s, respectively ($P^{spi}<0.01$ and $P^{Col4a1}<0.0005$; Figs. 3A-H, S3F). Col4a1 is thought to activate MAPK signalling through its putative receptor, the Discoidin domain receptor (Ddr)[23]. We used an enhancer trap in the *Ddr* locus and observed that *Ddr* was expressed in LPCs (Fig. S3K).

Spi activates EGFR[23], which was shown to be expressed in LPCs[12]. We ruled out the trivial explanation that the rescue of L5 numbers by Spi was caused by autocrine EGFR reactivation in the xg^O, as Spi expression in xg^O did not autonomously rescue dpMAPK nuclear localisation when EGFR signalling was blocked (Fig. S3L). To test whether *spi* expression in xg^O was indeed regulated by EGFR signalling, we measured *spi* mRNA levels using *in situ* hybridisation chain reaction. Disrupting EGFR signalling in xg^O resulted in significantly reduced fluorescence signal for *spi* mRNA in xg^O compared with controls (Figs. S3M-O; $P<0.01$). Thus, xg^O express *spi* in response to EGFR activity. Moreover, expressing *spi* or *Col4a1* in xg^O in which EGFR signalling was blocked rescued dpMAPK signal in L5s (Fig. S3P,Q), indicating that these ligands, when expressed from xg^O are sufficient to activate MAPK signalling in the rescued L5s.

Next, we tested whether Spi or Col4a1 could induce ectopic L5 differentiation when overexpressed in the xg^O. Expression of either ligand resulted in a 47.6% ±3 ($P<0.0001$) and 12.6% ±4 ($P<0.01$) increase in the number of L5s/column for Spi and Col4a1, respectively (Fig. 3I-K). Thus, Spi and Col4a1 are each sufficient to induce ectopic L5 differentiation when overexpressed in the xg^O. Given these results, we wondered why expressing either factor alone resulted in an incomplete rescue of L5 differentiation when EGFR was blocked in xg^O. We speculated that expressing Spi or Col4a1 alone may not lead to sufficiently high levels of MAPK activity in the proximal lamina. Therefore, we expressed both ligands together to assay whether they could rescue L5 differentiation when EGFR signalling was blocked in xg^O. Strikingly, this led to an enhanced and statistically significant rescue relative to expressing either one alone, resulting in laminas with 31.2% ±2.9 of the control number of L5s ($P<0.0001$; Figs. 3L-P).

Altogether, we find that xg^O secrete multiple factors that lead to activation of the MAPK cascade to induce differentiation of L5s in the proximal lamina.

Newly born L5 neurons inhibit differentiation of distal neighbours to set neuronal number

Although two rows of LPCs are specified as L5s, signals from the xg^O induce only the most proximal row to differentiate, ensuring that exactly one L5 is present in each lamina column. How this tight control of neuronal number is achieved is perplexing given that xg^O induce differentiation by secreting diffusible factors. The row of LPCs fated to differentiate into L5s is the row nearest to xg^O, and therefore, the first to receive differentiation signals. We speculated that these newly-induced L5s may then limit the ability of more distal LPCs to differentiate, by preventing MAPK activation in neighbouring cells. To test this hypothesis, we examined *argos* (*aos*) expression. Aos is a secreted antagonist of EGFR signalling, and transcriptional target of the pathway[16,24]. An enhancer trap in the *aos* locus, aos^{W11} was expressed in xg^O and differentiating L-neurons, with the highest levels detected in L5s (Fig. 4A). Interestingly, we also noted ectopic L5s in the laminas of aos^{W11} heterozygotes, which could be the result of decreased Aos expression, as aos^{W11} is a hypomorphic loss-of-function allele (Fig. 4A). These observations suggested that Aos could act in L5s as a feedback-induced sink for EGF ligands to limit further differentiation in the columns. To test this hypothesis, we knocked down *aos* by RNAi using a driver expressed in developing L5s specifically[25] (Fig. 4B). We observed a statistically significant ~1.2-fold increase in the number of L5s (Fig. 4C-E; $P<0.0005$). Thus, xg^O induce MAPK activity in the most proximal LPCs, resulting in their differentiation and in the production of the feedback inhibitor Aos. In turn, Aos limits further differentiation in the column by fine-tuning the availability of the differentiation signal Spi, which ensures that only one L5 differentiates per column, and determines the final number of neurons in each lamina column.

Discussion

Appropriate circuit formation and function require that neuronal numbers are tightly regulated. This is particularly important for the visual system, which is composed of repeated modular circuits spanning multiple processing layers. In *Drosophila,* photoreceptors induce their target field, the lamina, thus, establishing retinotopy between the compound eye and the lamina[8]. Each lamina unit or column in the adult is composed of exactly 5 neurons; however, columns

initially contain 6 LPCs. The sixth, or 'extra', LPC, invariantly located immediately distal to the differentiating L5 neuron, is fated to die by apoptosis. Here we show that these LPCs are specified as L5 neurons, effectively doubling the pool of LPCs that can give rise to L5s (Fig. 1). Our results imply that, rather than being naïve and equivalent, LPCs are pre-patterned according to their positions in columns, such that at least two populations of LPCs are present: proximal LPCs that are specified as L5s, and distal LPCs specified as L1-L4s.

The developmental strategies described thus far for setting neuronal number do so by regulating proliferation and/or survival[2]. Here, we have defined a unique strategy whereby L5 neuronal numbers are set by regulating how many precursors from a larger pool are induced to differentiate, followed by programmed cell death of the excess precursors. We showed that a glial population called xg^O, which are located proximal to the lamina, secrete at least two ligands (Spi, Col4a1) that activate MAPK signalling in LPCs to induce their differentiation (Fig. 3, S3). The tissue architecture is such that secreted signals from the xg^O reach the most proximal row of LPCs first, and therefore these precursors differentiate first. Upon differentiation, these newly induced neurons secrete the Spi antagonist Aos to limit the available pool of Spi and prevent further cells from differentiating (Figs. 4 and 5). Thus, the structure of the tissue together with feedback from newly induced neurons set neuronal number by limiting which and, therefore, how many LPCs are induced to differentiate.

Co-ordinating development through glia

We have shown that in addition to the wrapping glia[14], another population of glia, the xg^O, also receive and relay signals from photoreceptors to induce neuronal differentiation in the lamina (Fig. 2K-L). This is the first functional role ascribed to xg^O. Remarkably, xg^O are born from central brain DL1 type II neuroblasts and migrate into the optic lobes to positions below the developing lamina[26,27]. This underscores an extraordinary degree of coordination and interdependence between the compound eye, optic lobe and central brain. Photoreceptor signals drive wrapping glial morphogenesis and infiltration into the lamina[28], thus setting the pace of L1-L4 neuronal differentiation[14]. Defining the signals that enable xg^O to navigate the central brain and optic lobe will be a critical contribution to our understanding of how development is coordinated across brain regions.

Tissue architecture sets up stereotyped programmed cell death

In both vertebrate and invertebrate developing nervous systems, programmed cell death is thought to come in two broad flavours: first as an intrinsically programmed fate whereby specific lineages or identifiable progenitors, neurons or glia undergo stereotyped clearance[2,3,29,30], and second as an extrinsically controlled outcome of competition among neurons for limited target-derived trophic factors, which adjust overall cell numbers through stochastic clearance (also known as the neurotrophic theory)[2,3,30,31]. In the lamina, although the LPCs eliminated by programmed cell death are identifiable and the process stereotyped, it does not appear to be linked to an intrinsic programme. Rather, the predictable and stereotyped nature of apoptosis and differentiation are a consequence of stereotyped responses to extrinsic signalling determined by the architecture of the tissue. Thus, our work highlights that stereotyped patterns of apoptosis can arise from extrinsic signalling, suggesting a new mode to reliably pattern development of the nervous system.

In many contexts, neurotrophic factors promote cell survival by activating MAPK signalling[32,33]. In the lamina, MAPK-induced neuronal differentiation and cell survival appear intimately linked. LPCs that do not activate MAPK signalling sufficiently do not differentiate and are eliminated by apoptosis, likely through regulation of the proapoptotic factor Hid, which has been described extensively in flies[34–36]. Thus, here the xg^{O}-secreted ligands Spi and Col4a1, which activate MAPK, appear to be functioning as differentiation signals as well as trophic factors. Col4a1, in particular, may perform dual roles by promoting MAPK activity directly through its receptor Ddr, and perhaps also by limiting Spi diffusivity to aid in localising MAPK activation.

It will be interesting to determine whether the processes described here represent conserved strategies for regulating neuronal number. Certainly, given the diversity of cell types and structural complexity of vertebrate nervous systems, exploiting tissue architecture would appear to be an effective and elegant strategy to regulate cell numbers reliably and precisely.

Acknowledgements:

We thank C. Desplan, A. Gould, B. Shilo and J. Treisman for reagents, and S. Ackerman, M. Amoyel, B. Conradt, C. Desplan, C. Doe, A. Franz, P. Salinas, A. Rossi, C. Stern, L.

Venkatasubramanian and members of the Amoyel and Fernandes labs for comments on the manuscript. Stocks obtained from the Bloomington Drosophila Stock Center (NIH P40OD018537) were used in this study. Monoclonal antibodies obtained from the Developmental Studies Hybridoma Bank, created by the NICHD of the NIH and maintained at The University of Iowa, were used in this study.

Funding:

Wellcome Trust Sir Henry Dale Research Fellowship 210472/Z/18/Z (VMF), UCL Overseas Research Scholarship (ARP) and UCL Graduate Research Scholarship (ARP).

Author contributions:

Conceptualization: VMF, ARP, MPB

Investigation: ARP, MPB, ILB, ZH, VMF

Supervision: VMF

Writing – original draft: VMF

Writing – review & editing: ARP, MPB, ILB

Competing interests:

The authors declare no competing interests.

1 **Fig. 1**

2

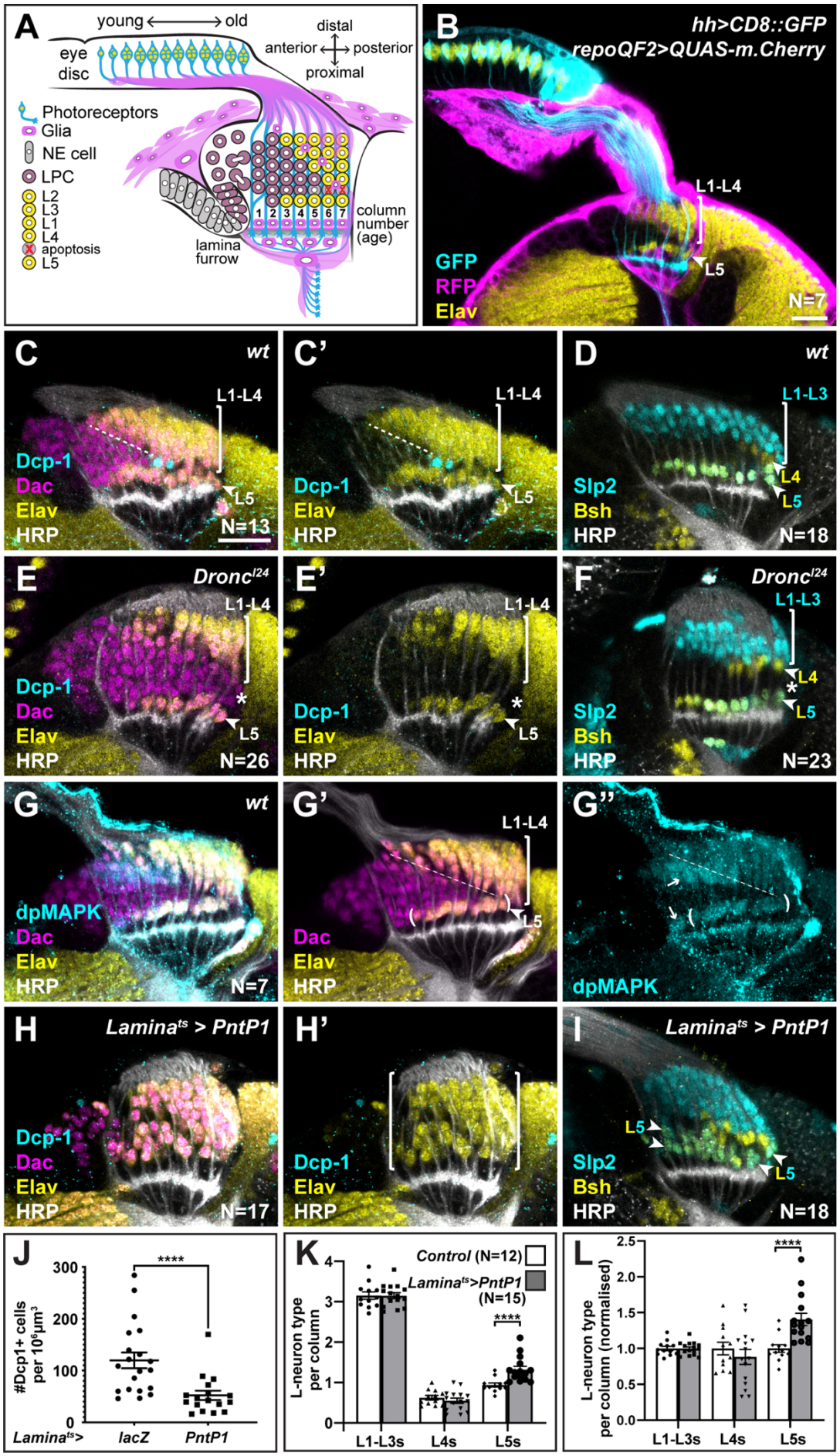
A
young
old
eye disc
distal
anterior
posterior
proximal
Photoreceptors
Glia
NE cell
LPC
L2
L3
L1
L4
apoptosis
L5
lamina furrow
1 2 3 4 5 6 7
column number (age)
B
hh>CD8::GFP
repoQF2>QUAS-m.Cherry
L1-L4
L5
GFP
RFP
Elav
N=7
C
wt
L1-L4
L5
Dcp-1
Dac
Elav
HRP
N=13
C'
L1-L4
L5
Dcp-1
Elav
HRP
D
wt
L1-L3
L4
L5
Slp2
Bsh
HRP
N=18
E
Dronc^I24
L1-L4
L5
Dcp-1
Dac
Elav
HRP
N=26
E'
L1-L4
L5
Dcp-1
Elav
HRP
F
Dronc^I24
L1-L3
L4
L5
Slp2
Bsh
HRP
N=23
G
wt
dpMAPK
Dac
Elav
HRP
N=7
G'
L1-L4
L5
Dac
Elav
HRP
G''
dpMAPK
H
Lamina^ts > PntP1
Dcp-1
Dac
Elav
HRP
N=17
H'
Dcp-1
Elav
HRP
I
Lamina^ts > PntP1
L5
L5
Slp2
Bsh
HRP
N=18
J
#Dcp1+ cells per 10^6 µm^3
300
200
100
0
****
Lamina^ts>
lacZ
PntP1
K
Control (N=12)
Lamina^ts>PntP1 (N=15)
L-neuron type per column
4
3
2
1
0
****
L1-L3s
L4s
L5s
L
L-neuron type per column (normalised)
2.5
2.0
1.5
1.0
0.5
0.0
****
L1-L3s
L4s
L5s

Fig. 1: The 'extra' LPCs are specified as L5s

(A) Schematic of the developing lamina. Photoreceptors (blue) drive lamina precursor cell (LPC; purple) birth from neuroepithelial cells (NE; grey) and their assembly into columns of ~6 LPCs, which differentiate into the L1-L5 neurons (yellow) following an invariant spatiotemporal pattern. The 'extra' LPC is cleared by apoptosis (red X). Several glial types (magenta) associate with the lamina. **(B)** A cross-sectional view of an early pupal (0-5 hours APF) optic lobe where *hh-Gal4* drives *UAS-CD8::GFP* expression in photoreceptors (cyan). The pan-glial driver *repo-QF2* drives *QUAS-m.Cherry* (magenta) in all glia. Elav (yellow) marks all neurons. **(C,D)** Wild-type optic lobes stained for **(C)** Dac (lamina cell bodies; magenta), Horseradish peroxidase (photoreceptor axons; HRP; white), Elav (neurons; yellow) and cleaved Dcp-1 (apoptotic cells; cyan). Dcp-1 positive cells are located between L1-L4s and L5s and correspond to the 'extra' LPCs, which are being eliminated. **(D)** HRP (white) and L-neuron subtype specific markers Slp2 (cyan) and Bsh (yellow), which individually mark L1-L3 and L4s respectively, and are co-expressed in L5s. **(E,F)** *Dronc*^{I24} optic lobes stained for the same markers as in (C) and (D), respectively. **(E)** No Dcp-1 positive cells were recovered and Dac positive cells between L1-L4s and L5s persisted into the oldest columns. **(F)** A space (negative for both markers; asterisk) was present between L4s and L5s. **(G)** Wild-type optic lobes stained for Dac (magenta), HRP (white), Elav (yellow) and dpMAPK (cyan). dpMAPK levels were high (arrows in G") just prior to Elav expression (dashed line for the front of L1-L4 differentiation and brackets for L5 differentiation). **(H,I)** Optic lobes with lamina-specific overexpression of PntP1 stained as in (C) and (D), respectively. **(H)** Fewer Dcp-1 positive cells were recovered compared with controls. **(I)** Roughly two rows of Slp2 and Bsh co-expressing cells (L5s) were recovered (arrow heads). **(J)** Quantification of the number of Dcp-1 positive cells in (H) compared with control *Lamina*^{ts}*>lacZ* (Figure S1A) ($P<0.0001$; Mann-Whitney U test; error bars indicate standard error of the mean; SEM). **(K)** Quantification of the number of L-neuron types per column based on Slp2 and Bsh expression from column 7 onwards shows an increase in the number of L5s/column in *Lamina*^{ts}*>PntP1* compared with controls; $P<0.0001$; Mann-Whitney U test. **(L)** Same as (K) but normalised to the mean of the control. The number of L5s/column in *Lamina*^{ts}*>PntP1* increase ~1.4 fold relative to controls; $P<0.0001$; Mann-Whitney U test. Error bars indicate SEM. Ns indicated in parentheses for J,K. Scale bar = 20µm.

1 **Fig. 2**

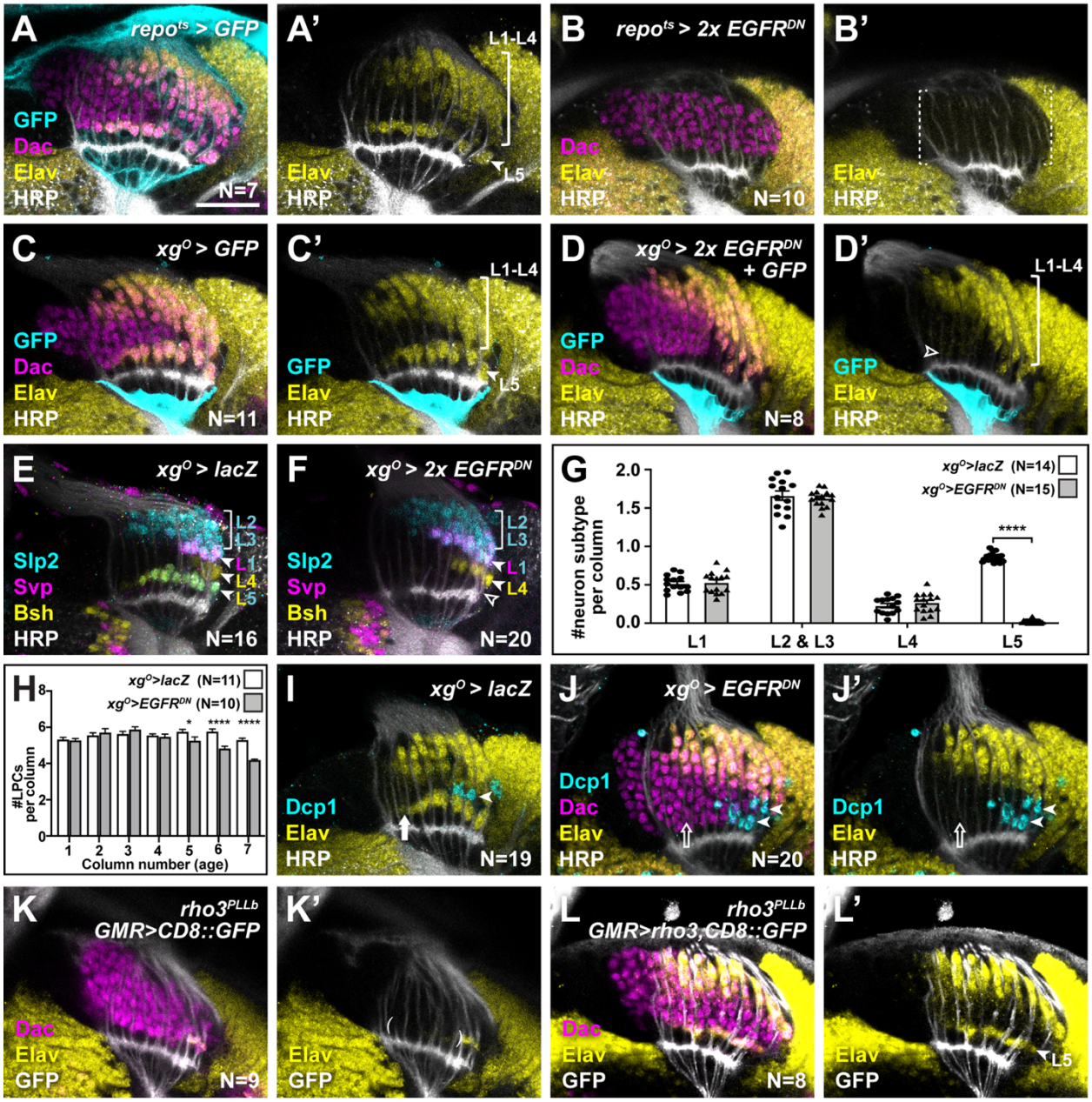
A
repo^ts > GFP
GFP
Dac
Elav
HRP
N=7
A'
L1-L4
L5
Elav
HRP
B
repo^ts > 2x EGFR^DN
Dac
Elav
HRP
N=10
B'
Elav
HRP
C
xg^O > GFP
GFP
Dac
Elav
HRP
N=11
C'
L1-L4
L5
GFP
Elav
HRP
D
xg^O > 2x EGFR^DN + GFP
GFP
Dac
Elav
HRP
N=8
D'
L1-L4
GFP
Elav
HRP
E
xg^O > lacZ
L2
L3
L1
L4
L5
Slp2
Svp
Bsh
HRP
N=16
F
xg^O > 2x EGFR^DN
L2
L3
L1
L4
Slp2
Svp
Bsh
HRP
N=20
G
xg^O>lacZ (N=14)
xg^O>EGFR^DN (N=15)
#neuron subtype per column
2.0
1.5
1.0
0.5
0.0
****
L1
L2 & L3
L4
L5
H
xg^O>lacZ (N=11)
xg^O>EGFR^DN (N=10)
#LPCs per column
8
6
4
2
0
*
****
****
1
2
3
4
5
6
7
Column number (age)
I
xg^O > lacZ
Dcp1
Elav
HRP
N=19
J
xg^O > EGFR^DN
Dcp1
Dac
Elav
HRP
N=20
J'
Dcp1
Elav
HRP
K
rho3^PLLb
GMR>CD8::GFP
Dac
Elav
GFP
N=9
K'
Elav
GFP
L
rho3^PLLb
GMR>rho3,CD8::GFP
Dac
Elav
GFP
N=8
L'
Elav
GFP
L5

2

Fig. 2: Outer chiasm giant glia induce L5 neuronal differentiation in response to EGF from photoreceptors

(A) A cross-sectional view of an optic lobe with pan-glial expression of CD8::GFP stained for GFP (cyan), Dac (magenta), Elav (yellow) and HRP (white). **(B)** Pan-glial expression of 2 copies of $EGFR^{DN}$ stained for Dac (magenta), Elav (yellow) and HRP (white). Although LPCs (Dac+ cells) formed, they did not differentiate (lack of Elav+ cells). **(C)** xg^{O}-specific expression of CD8::GFP stained for GFP (cyan), Dac (magenta), Elav (yellow) and HRP (white). **(D)** xg^{O}-specific expression of 2 copies of $EGFR^{DN}$ and CD8::GFP stained for GFP (cyan), Dac (magenta), Elav (yellow) and HRP (white). The number of Elav+ cells in proximal row (L5s) was decreased (empty arrowhead). **(E,F)** HRP (white) and L-neuron subtype specific markers Slp2 (cyan), Bsh (yellow) and Svp (magenta) in **(E)** Control $xg^{O}>lacZ$ optic lobe and **(F)** $xg^{O}>2xEGFR^{DN}$. The number of cells co-expressing Slp2 and Bsh (L5s) was reduced. **(G)** Quantification of the number of L-neuron subtypes per column for control and $xg^{O}>2xEGFR^{DN}$. Only L5 neurons were decreased significantly ($P^{L5}<0.0001$; Mann-Whitney U test. Error bars indicate SEM. Ns indicated in parentheses). **(H)** Quantification of the number of LPCs/column (*i.e.* Dac+ cells/column) for control and $xg^{O}>2xEGFR^{DN}$ showed that a significant decrease was observed only from column 5 onwards (P*<0.05, P****<0.0002; Mann-Whitney U test. Error bars indicate SEM. Ns indicated in parentheses). **(I)** Control $xg^{O}>lacZ$ optic lobe stained for Dcp-1 (cyan), Elav (yellow) and HRP (white). Dcp-1+ cells were always observed just distal to the most proximal row of cells (L5s). **(J)** $xg^{O}>EGFR^{DN}$ stained for Dcp-1 (cyan), Dac (magenta) Elav (yellow) and HRP (white). Dcp-1 positive cells were observed in the most proximal row of LPCs as well as the row just distal to these, starting from column 5.93 ±0.18SEM. **(K)** GMR-Gal4 driven CD8::GFP expression in photoreceptors in a $rho3^{PLLb}$ background stained for GFP (white), Dac (magenta), Elav (yellow). Few proximal Elav+ cells (L5s) were recovered in older columns only as previously published [14]. **(L)** GMR-Gal4 driven Rho3 and CD8::GFP in a $rho3^{PLLb}$ background stained for GFP (white), Dac (magenta), Elav (yellow) showed that L5 neuronal differentiation was rescued (Elav+ cells in the proximal lamina). Scale bar = 20µm.

1 **Fig. 3**

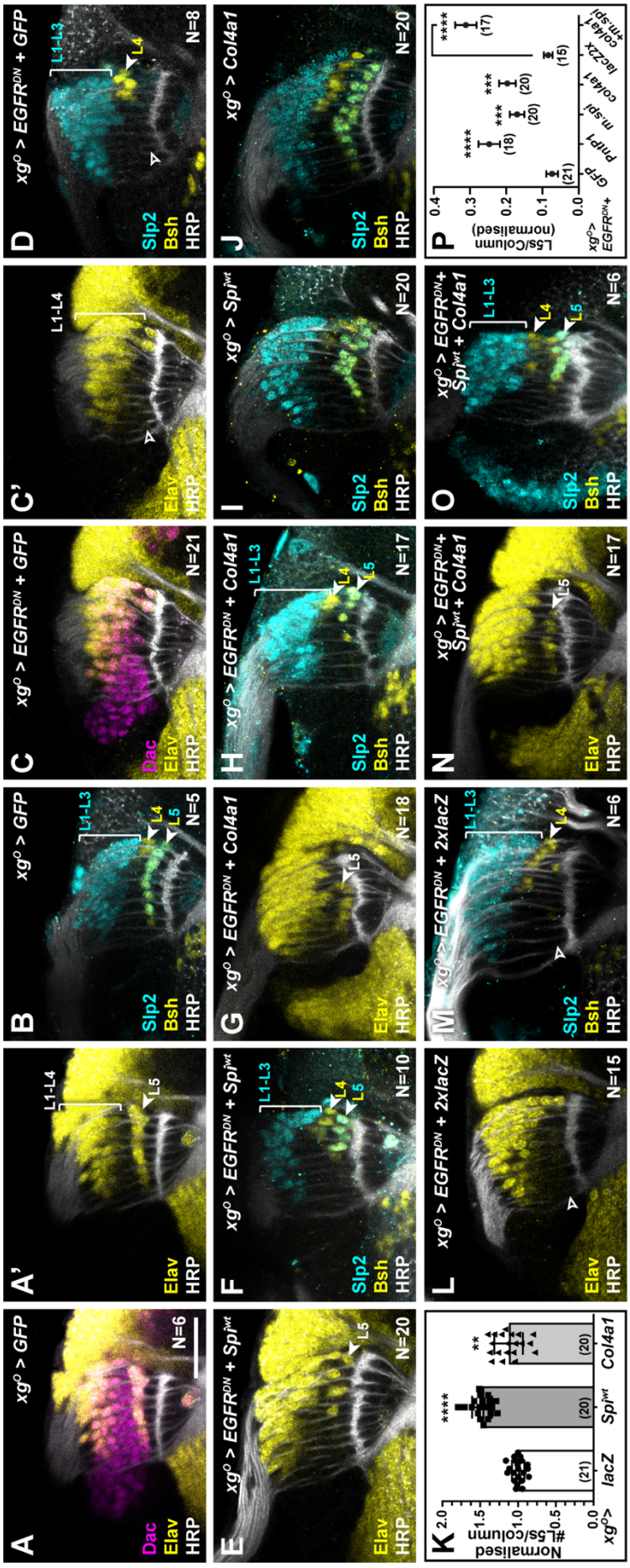
A
xg^O > GFP
Dac
Elav
HRP
N=6
A'
L1-L4
L5
Elav
HRP
B
xg^O > GFP
L1-L3
L4
L5
Slp2
Bsh
HRP
N=5
C
xg^O > EGFR^DN + GFP
Dac
Elav
HRP
N=21
C'
L1-L4
Elav
HRP
D
xg^O > EGFR^DN + GFP
L1-L3
L4
Slp2
Bsh
HRP
N=8
E
xg^O > EGFR^DN + Spi^wt
L5
Elav
HRP
N=20
F
xg^O > EGFR^DN + Spi^wt
L1-L3
L4
L5
Slp2
Bsh
HRP
N=10
G
xg^O > EGFR^DN + Col4a1
L5
Elav
HRP
N=18
H
xg^O > EGFR^DN + Col4a1
L1-L3
L4
L5
Slp2
Bsh
HRP
N=17
I
xg^O > Spi^wt
Slp2
Bsh
HRP
N=20
J
xg^O > Col4a1
Slp2
Bsh
HRP
N=20
K
Normalised #L5/column
2.0
1.5
1.0
0.5
0.0
****
**
(21)
(20)
(20)
xg^O>
lacZ
Spi^wt
Col4a1
L
xg^O > EGFR^DN + 2xlacZ
Elav
HRP
N=15
M
xg^O > EGFR^DN + 2xlacZ
L1-L3
L4
Slp2
Bsh
HRP
N=6
N
xg^O > EGFR^DN+ Spi^wt + Col4a1
L5
Elav
HRP
N=17
O
xg^O > EGFR^DN+ Spi^wt + Col4a1
L1-L3
L4
L5
Slp2
Bsh
HRP
N=6
P
L5s/column (normalised)
0.4
0.3
0.2
0.1
0.0
****
***
***
****
(21)
(18)
(20)
(20)
(15)
(17)
xg^O> EGFR^DN+
GFP
Pnlp1
m-spi
Col4a1
lacZ2x
Col4a1 +m-spi

Fig. 3: Xg^O secrete multiple ligands to induce L5 neuronal differentiation

(A,B) Control *xg^O>GFP* optic lobes. **(A)** Dac (magenta), Elav (yellow) and HRP (white) or **(B)** HRP (white) and L-neuron specific markers Slp2 (cyan) and Bsh (yellow). **(C,D)** Gal4 titration control *xg^O>GFP+$EGFR^{DN}$* **(C)** Dac (magenta), Elav (yellow) and HRP (white). Elav+ cells were reduced in number in the proximal lamina. **(D)** HRP (white) and L-neuron specific markers Slp2 (cyan) and Bsh (yellow). The number of Slp2 and Bsh co-expressing cells was reduced. **(E,F)** Wild-type Spi (Spi^{wt}) co-expression with $EGFR^{DN}$ specifically in xg^O. **(E)** stained for Elav (yellow) and HRP (white). Some Elav+ cells were recovered in the proximal lamina **(F)** HRP (white) and L-neuron specific markers Slp2 (cyan) and Bsh (yellow). Slp2 and Bsh co-expressing cells were recovered in the proximal lamina. **(G,H)** Col4a1 co-expression with $EGFR^{DN}$ specifically in xg^O. **(G)** stained for Elav (yellow) and HRP (white). Some Elav+ cells were recovered in the proximal lamina **(H)** HRP (white) and L-neuron specific markers Slp2 (cyan) and Bsh (yellow). Slp2 and Bsh co-expressing cells were recovered in the proximal lamina. **(I,J)** Optic lobes stained for Slp2 and Bsh when xg^O overexpress **(I)** Spi^{wt} or **(J)** Col4a1. In both instances, ectopic Slp2 and Bsh co-expressing cells (L5s) are recovered in the proximal lamina. **(K)** Quantification of the number of L5s/column from (I-J) normalised to the control *xg^O>lacZ*. ($P^{spi.wt}$<0.0001; P^{Col4a1}<0.01; Mann-Whitney U test. Error bars indicate SEM. Ns indicated in parentheses). **(L,M)** Gal4 titration control *xg^O>$EGFR^{DN}$+2xlacZ* stained for **(L)** Elav (yellow) and HRP (white) or **(M)** HRP (white), Slp2 (cyan) and Bsh (yellow). **(N,O)** Wild-type Spi^{wt} and Col4a1 co-expression with $EGFR^{DN}$ specifically in xg^O. **(N)** stained for Elav (yellow) and HRP (white). Elav+ cells were recovered in the proximal lamina **(O)** HRP (white) and L-neuron specific markers Slp2 (cyan) and Bsh (yellow). Slp2 and Bsh co-expressing cells were recovered in the proximal lamina. **(P)** Quantification of the number of L5s/column for the genotypes indicated normalised to the appropriate titration control *xg^O>lacZ.* (P^{***}<0.0005; P^{****}<0.0001; Mann-Whitney U test. Error bars indicate SEM. Ns indicated in parentheses). Scale bar = 20µm.

1 **Fig. 4**

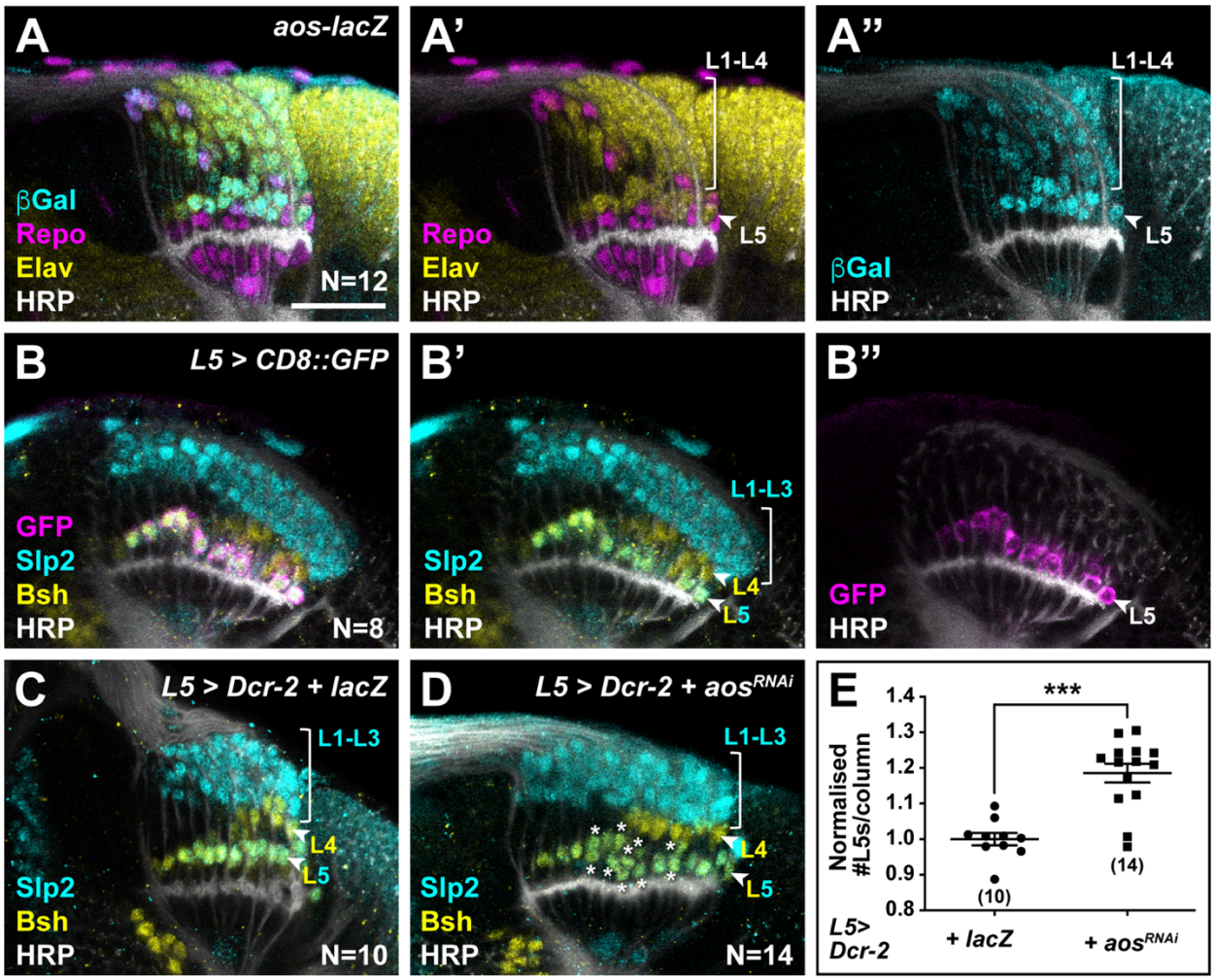
A
aos-lacZ
βGal
Repo
Elav
HRP
N=12
A'
L1-L4
L5
Repo
Elav
HRP
A''
L1-L4
L5
βGal
HRP
B
L5 > CD8::GFP
GFP
Slp2
Bsh
HRP
N=8
B'
L1-L3
L4
L5
Slp2
Bsh
HRP
B''
GFP
HRP
L5
C
L5 > Dcr-2 + lacZ
L1-L3
L4
L5
Slp2
Bsh
HRP
N=10
D
L5 > Dcr-2 + aosRNAi
L1-L3
L4
L5
Slp2
Bsh
HRP
N=14
E
***
Normalised #L5s/column
1.4
1.3
1.2
1.1
1.0
0.9
0.8
(10)
(14)
L5> Dcr-2
+ lacZ
+ aosRNAi

2

Fig. 4: Newly-induced L5 neurons secrete Aos to limit inductive signals from xg^O

(A) *aos-lacZ* expression in the lamina with β-Gal (cyan), Repo (magenta), Elav (yellow), HRP (white). The highest levels of β-Gal expression were observed in proximal LPCs (L5s). Ectopic Elav+ cells were observed in the proximal lamina. **(B)** An L5-specific Gal4 was used to drive GFP (magenta) expression in the lamina; HRP (white) and L-neuron subtypes Slp2 (cyan) and Bsh (yellow). GFP was observed specifically in Slp2 and Bsh co-expressing cells (L5s) with low levels in the youngest neurons. **(C,D)** Optic lobes stained for HRP (white), Slp2 (cyan) and Bsh (yellow) in **(C)** Control *L5>Dcr-2+lacZ* and **(D)** when Dcr-2 and aos^{RNAi} were expressed in developing L5 neurons specifically, which led to an increase in the number of Slp2 and Bsh co-expressing cells (L5s). **(E)** Quantification of the number of L5s/column normalised for (D) and (E) normalised to control (D). (P***<0.0005; Mann-Whitney U test. Error bars indicate SEM. Ns indicated in parentheses). Scale bar = 20µm.

1 **Fig. 5**

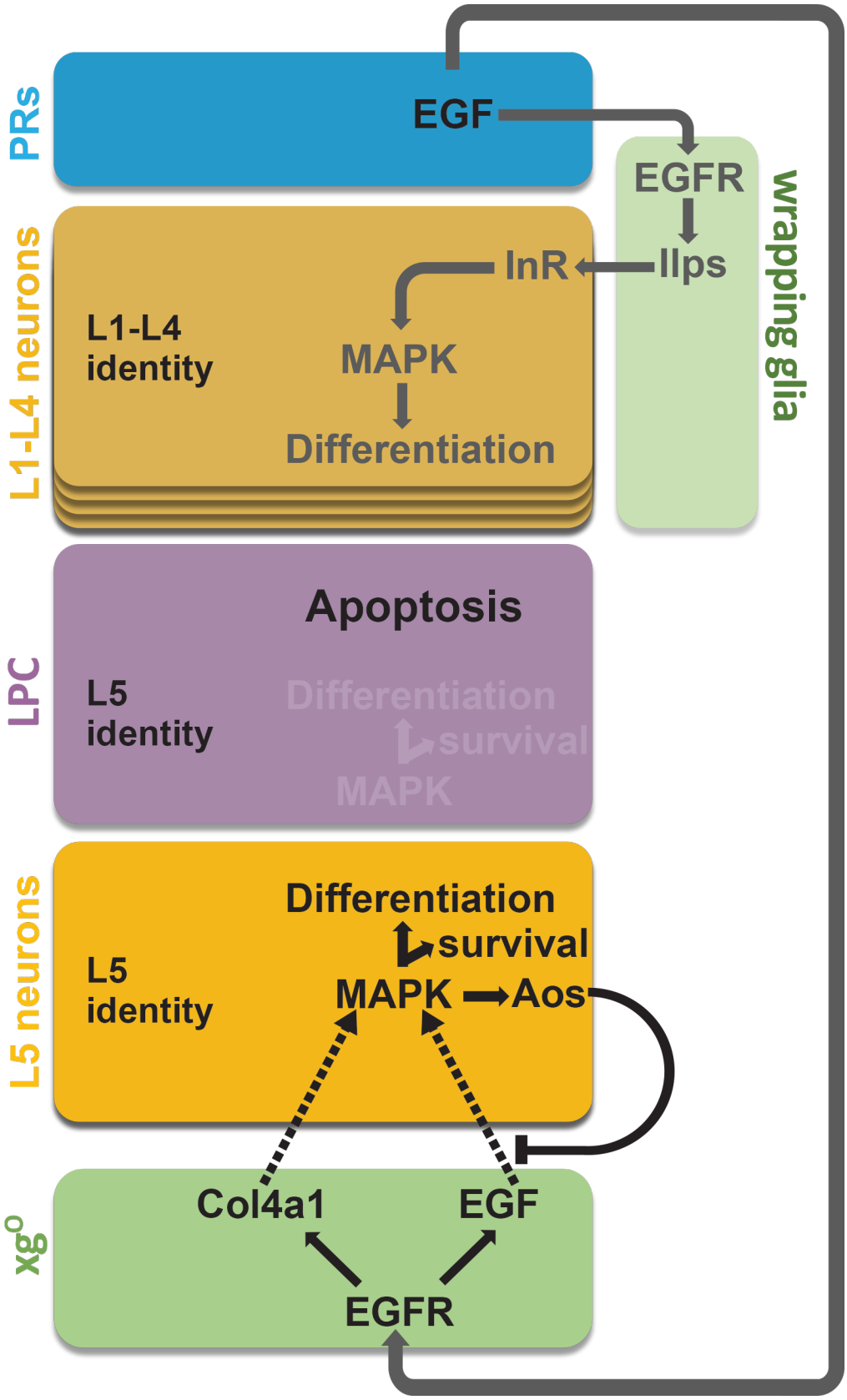
PRs
EGF
EGFR
Ilps
wrapping glia
L1-L4 neurons
L1-L4
identity
InR
MAPK
Differentiation
LPC
L5
identity
Apoptosis
Differentiation
survival
MAPK
L5 neurons
L5
identity
Differentiation
survival
MAPK
Aos
xg0
Col4a1
EGF
EGFR

2

Fig. 5: Summary schematic of neuronal differentiation in the lamina

In our model of lamina neuronal differentiation, lamina precursor cells are prepatterned with unique identities based on their positions within a column, such that the two most proximal cells are specified with L5 identity. EGF from photoreceptors activates EGFR signalling in wrapping glia, which induce L1-L4 differentiation, and in xg^{O}, which induce L5 differentiation. Only a subset of the LPCs specified as L5s differentiate (*i.e.* those in the proximal row). We propose that this selective neuronal induction of L5s is due to tissue architecture and feedback from the newly born L5s, which limit available EGF (Spi) by secreting the antagonist Aos.

Materials and Methods

<u>*Drosophila stocks and maintenance:*</u>

Drosophila melanogaster strains and crosses were reared on standard cornmeal medium and raised at 25°C or 29°C or shifted from 18°C to 29°C for genotypes with temperature sensitive Gal80, as indicated in Table S2.

We used the following mutant and transgenic flies in combination or recombined in this study (See Table S2 for more details; {} enclose individual genotypes, separated by commas): *{y,w,hsflp^{122}; sp/Cyo; TM2/TM6B}, {y,w; sp/Cyo, Bacc-GFP; Dr/TM6C},* (from BDSC: 36349) *{ey-Gal80; sp/Cyo;}* (BDSC: 35822), *{;Gal80^{ts}; TM2/TM6B}* (BDSC: 7108), *{w^{1118};; R27G05-Gal4}* (BDSC: 48073), *{w^{1118};;25A01-Gal4}* (BDSC: 49102), *{y,w; R64B07-Gal4;}* (larval L5-Gal4), {y,w; hh-Gal4/TM3} (BDSC: 67493), *{;tub-Gal80^{ts}; repo-Gal4/TM6B}, {w^{1118};GMR-Gal4/Cyo;}* (BDSC: 9146), *{y,w;Pin/Cyo;repo-QF/TM6B}* (BDSC: 66477), *{y,w; NP6293-Gal4/Cyo,UAS-lacZ;}* (perineurial glia; Kyoto Stock Center: 105188), *{w; NP2276-Gal4/Cyo; }* (subperineurial glia; Kyoto Stock Center: 112853)*, {w^{1118};; R54H02-Gal4}* (cortex glia; BDSC: 45784), *{w^{1118};; R10C12-Gal4}* (epithelial and marginal glia; BDSC: 47841), *{w;Mz97-Gal4, UAS-Stinger/Cyo;}* (wrapping and xg^{O}; BDSC: 9488), *{w^{1118};; R53H12-Gal4}* (chiasm glia; BDSC: 50456), *{y,w; spi^{NP0289}-Gal4/Cyo, UAS-lacZ;}* (Kyoto Stock Center: 112128), *{w^{1118}; Cg-Gal4;}* (BDSC: 7011), *{w;; bnl^{NP2211}-Gal4}* (Kyoto Stock Center: 112825), *{w; ths^{MI07139}-Gal4/Cyo; MKRS/TM6B}* (BDSC: 77475), *{;;rho3^{PLLb}, UAS-CD8::GFP/TM6B}, {;UAS-rho3-3xHA;}* (gifts from B. Shilo), *{;;aos^{w11}/TM6B}* (*aos-lacZ*; BDSC: 2513), *{y,w; sp/Cyo, Bacc-GFP; 10xQUAS-6xmCherry-HA}* (BDSC: 52270), *{y,w;;10xUAS-myrGFP}* (BDSC: 32197), *{;UAS-CD8::GFP;}, {;;UAS-CD8::GFP}* (gifts from C. Desplan)*, {y,w;;UAS-nls.lacZ},* (BDSC: 3956)*, {y,w; UAS-LifeAct-GFP/Cyo;}* (BDSC: 35544)*, {w^{1118};UAS-Dcr-2;}* (BDSC: 24650), *{w^{1118};;UAS-Dcr-2}* (BDSC: 24651), *{;UAS-EGFR^{DN}; UAS-EGFR^{DN}}* (BDSC: 5364)*, {;UAS-aop^{ACT};}* (Kyoto Stock Center: 108425), *{y,w;UAS-rl^{sem};}* (rl^{sem} = MAPK^{ACT}; BDSC: 59006), *{w^{1118};;UAS-PntP1}* (BDSC: 869), *{w^{1118};UAS-aos^{RNAi};}* (VDRC47181), *{w;UAS-jeb;}* (a gift from A. Gould), *{y,w, UAS-Col4a1^{EY11094}/(Cyo);}* (BDSC: 20661), *{;;UAS-Cg25c-RFP}* [37] *(Col4a1 = Cg25c)*, *{;UAS-Wnt5;}* (BDSC: 64298), *{;;UAS-s.spi}* (a gift from B. Shilo), *{;UAS-m.spi::GFP-myc;}* (a gift from B. Shilo), *{;;UAS-m.spi::GFP-myc}* (a gift from B. Shilo), *{w, UAS-grk.sec/Cyo;}* (BDSC: 58417), *{;UAS-vn^{EPgy}/Cyo;}* (BDSC: 58498), *{;;UAS-krn-3xHA}* (FlyORF: F002754), *{;UAS-bnl/Cyo; MKRS/TM6C}* (BDSC: 64232), *{;UAS-Ilp1;}, {;UAS-*

Ilp6;} (gifts from P. Leopold), *{w^{1118}, UAS-Pvf1^{XP};;}* (BDSC: 19632), *{w^{1118}; UAS-Pvf2^{XP};}* (BDSC: 19631), *{;UAS-Wnt4^{EPgy2}/Cyo;}* (BDSC: 20162), *{;;UAS-boss-3xHA}* (FlyORF: F001365), *{y,sev; SAM.dCas9.Trk;}* (BDSC: 81322), *{y,sev; SAM.dCas9.Pvf3;}* (BDSC: 81346), *{y,sev; SAM.dCas9.ths;}* (BDSC: 81347), *{y,sev; SAM.dCas9.pyr;}* (BDSC: 81330), *{w^{1118}; Ddr^{CR01018}-Gal4;}* (BDSC: 81157).

Mosaic analysis:

We induced *Dronc^{I24}* MARCM clones (Fig. S3C) and *Dronc^{I24}, UAS-Yan^{ACT}* MARCM clones (Fig. S3D) by heat-shocking larvae (2 days AEL) for 120 minutes at 37ºC. All MARCM crosses were raised at 25ºC until dissection at 0-5 hours APF.

Immunocytochemistry, in situ hybridization chain reaction, antibodies and microscopy:

We dissected eye-optic lobe complexes from early pupae (0-5hrs APF) in 1X phosphate-buffered saline (PBS), fixed in 4% formaldehyde for 20 minutes, blocked in 5% normal donkey serum and incubated in primary antibodies diluted in block for 2 nights at 4ºC. Samples were then washed in 1X PBS with 0.5% TritonX (PBSTx), incubated in secondary antibodies diluted in block, washed in PBSTx and mounted in SlowFade (Life Technologies).

When performing phospho-MAPK stains, dissections were performed in a phosphatase inhibitor buffer as detailed in [38].

To detect *spi* transcripts by *in situ* hybridization chain reaction, we dissected, fixed and permeabilized the optic lobes as above before following the protocol described in [39].

We used the following primary antibodies in this study: mouse anti-Dac$^{2-3}$ (1:20, Developmental Studies Hybridoma Bank; DSHB), mouse anti-Repo (1:20, DSHB), rat anti-Elav (1:100, DSHB), mouse anti-Elav (1:20, DSHB), rabbit anti-Dcp-1 (1:100; Cell Signalling #9578), chicken anti-GFP (1:400; EMD Millipore), mouse anti-Svp (1:50, DSHB), rabbit anti-Slp2 (1:100; a gift from C. Desplan), rabbit-Bsh (1:500; a gift from C. Desplan), Rat anti-Pdm3 (1:1000; a gift from C. Desplan), guinea pig anti-Brp (1:100; a gift from C. Desplan), rabbit anti-Phospho-p44/42 MAPK (Erk1/2) (Thr202/Tyr204) (1:100, Cell Signaling #9101), chicken anti-RFP (1:500; Rockland #600-901-379s), mouse anti β-galactosidase (1:500; Promega # Z3781), chicken anti

β-galactosidase (1:500; abcam #9361), rabbit-anti-GFP (1:500; Thermofisher #A6455), AlexaFluor405 conjugated Goat Anti-HRP (1:100; Jackson Immunolabs), AlexaFluor405-, Cy3-, or AlexaFluor647- conjugated Goat Anti-HRP (1:200; Jackson Immunolabs). Secondary antibodies were obtained from Jackson Immunolabs or Invitrogen and used at 1:800. Images were acquired using Zeiss 800 and 880 confocal microscopes with 40X objectives.

Quantification and Statistical analyses:

We used Fiji-ImageJ [40] or Imaris (version x64-9.5.1) to process and quantify confocal images as described below. We used Adobe Photoshop and Adobe Illustrator software to prepare figures. We used GraphPad Prism8 to perform statistical tests. In all graphs, whiskers indicate the standard error of the mean (SEM).

Dcp-1 quantifications:

We used the surfaces tool in Imaris to manually select the lamina region (based on Dac expression). We then used the spots tool to identify Dcp-1 positive cells (cell diameter = 5μm) within the selected region using the default thresholding settings, and plotted these values normalised to the volume of the selected lamina region in GraphPad Prism8.

Cell-type quantifications:

LPCs per column: Column number was identified by counting HRP-labelled photoreceptor axon bundles. We considered the youngest column located adjacent to the lamina furrow to be the first column, with column number (age) increasing towards the posterior (right) of the furrow. We counted the number of Dac+ cells per column by quantifying 10 optical slices (step size = 1μm) located centrally in the lamina.

Control vs. *Lamina^{ts}>PntP1:* We quantified the lamina neuron subtypes per column using the following markers to identify L-neuron types: Elav+ and Slp2+ cells were counted as L1-L3s; Elav+ and Bsh+ cells were counted as L4s and Elav+, Bsh+ and Slp2+ cells were counted as L5s. We quantified 10 optical slices (step size = 1μm) located centrally in the lamina. Column number was identified by counting HRP-labelled photoreceptor axon bundles. These quantifications were done blind.

Ligand receptor screen: We quantified the number of L5s based on Elav expression in the proximal lamina. Column number was identified by counting HRP-labelled photoreceptor axon bundles. We quantified 30 optical slices (step size = 1μm) located centrally in the lamina.

Ligand over-expression quantifications: We quantified the number of L-neuron types per column using Elav, Bsh and Slp2. We quantified 30 optical slices (step size = 1μm) located centrally in the lamina. Column number was identified by counting HRP-labelled photoreceptor axon bundles.

Spi Probe Intensity Quantifications:
In Fiji-ImageJ we used the free hand selection tool to draw a region of interest (ROI) around the xg^O (marked by the *xg^O>CD8::GFP*). We then measured the mean fluorescence intensity of *spi* transcripts labelled by HCR within each ROI. We quantified 30 optical slices (step size = 1μm) located centrally in the lamina and then plotted the average for each optic lobe.

Number of xg^O:
We quantified the number of xg^O (Fig. S2Q) by manually counting the number of Repo positive nuclei within LifeAct-GFP positive xg^O per 40μm optical section in Fiji-ImageJ. We used a step size of 1mm while acquiring the z-stacks and centred each 40μm optical section in the middle of the lamina using photoreceptor axons (HRP), and the lobula plug (Dac expression) as landmarks. Quantifications were performed blind.

Length of xg^O processes:
We quantified the lengths of the fine glial processes that extend distally from the xg^O towards the lamina plexus (Fig. S2O,P,R) by using the straight-line selection and measuring tools in Fiji-ImageJ to measure xg^O process lengths in a 10mm optical section centred in the middle of the lamina. Quantifications were performed blind.

dpMAPK quantifications nuclear to cytoplasmic:
Using Fiji we manually drew regions of interest (ROIs) with the free hand selection tool around the xg^O nucleus (based on Repo) and added these to the ROI manager. We then enlarged the

ROIs (Edit>Selection>Enlarge) by 3.00 pixel units to include the cytoplasm. We then used the XOR function in the ROI Manager to only select the cytoplasm of the xg^O. We then measured the MFI of dpMAPK in the nucleus and the cytoplasm of the xg^O in 20 centrally located optical slices (corresponding to 20μm) for each optic lobe. We plotted the nuclear:cytoplasmic ratios of dpMAPK MFI in GraphPad Prism8.

Supplemental Information

Supplementary text

EGFR activity is required in xg^O for L5 differentiation specifically during lamina development

Blocking EGFR in xg^O throughout development led to a dramatic decrease in putative L5 neurons (Elav+ cells in the proximal lamina). To rule out that the reduction in proximal Elav-positive cells was due to EGFR playing a role in early development of the xg^O, we used $Gal80^{ts}$ to restrict $EGFR^{DN}$ expression in xg^O to only the 3rd larval instar, when lamina development occurs. This resulted in a similar loss of Elav-positive cells in the proximal lamina as when continuously expressing $EGFR^{DN}$ in the xg^O, indicating that this phenotype is not due to an early defect in xg^O (Fig. S2N).

MAPK activity is necessary and sufficient for L5 neuronal differentiation

We tested whether MAPK signalling is required for L5 differentiation, by expressing a dominant active form of the transcriptional repressor Anterior open (Aop^{ACT}) to block transcription downstream of MAPK in the lamina[41]. As reported previously, this resulted in small laminas with few LPCs, and very few to no differentiated neurons (Fig. S3A,B; N=7)[14]. MAPK signalling is often required for cell survival[34–36] and indeed we observed cleaved Dcp-1 in LPCs prior to column formation (Fig. S3B). To bypass this LPC survival defect and probe the effects of disrupting MAPK signalling on L5 differentiation, we generated clones homozygous mutant for *Dronc* that expressed UAS-Aop^{ACT}, thus blocking apoptosis while mis-expressing Aop^{ACT}. These clones were recovered with very low frequency compared with *Dronc* mutant clones alone and were recovered in the lamina even less frequently. Nonetheless, we found that although these clones contained LPCs, they did not contain any differentiated neurons (Elav+ cells), including at proximal positions where L5s normally differentiate (Fig. S3D). Thus, MAPK

signalling is both necessary and sufficient to induce neuronal differentiation of L5s, and reducing MAPK activity results in death of LPCs.

Eliminating false positive hits from the xg^O rescue screen

To identify the signal(s) secreted by xg^O that induce L5 neuronal differentiation, we screened 18 MAPK-activating ligands for their ability to rescue the loss of Elav expression in the proximal lamina when co-expressed with $EGFR^{DN}$ in the xg^O (Fig. S3F). Of these, Spitz (Spi) Branchless (Bnl), Thisbe (Ths) and Collagen type IV alpha 1 (Col4a1) produced statistically significant rescues when compared with the *xg^O>$EGFR^{DN}$+CD8::GFP* (Gal4 titration control) (Fig. S3F). To eliminate false positive hits, we examined available enhancer trap lines and published reports to determine whether xg^O express these ligands under physiological conditions. We found that: spi^{NP0289}, a Gal4 insertion into the Spi locus and Collagen-Gal4 (Cg-Gal4)[42] both drove expression of UAS-CD8::GFP in xg^O (Figs. S4G-I). However, bnl-Gal4[43] drove expression ubiquitously in all cells of the optic lobe, making it unlikely to be a viable hit, while ths-Gal4 only drove expression in photoreceptors and not xg^O.

1 **Fig. S1**

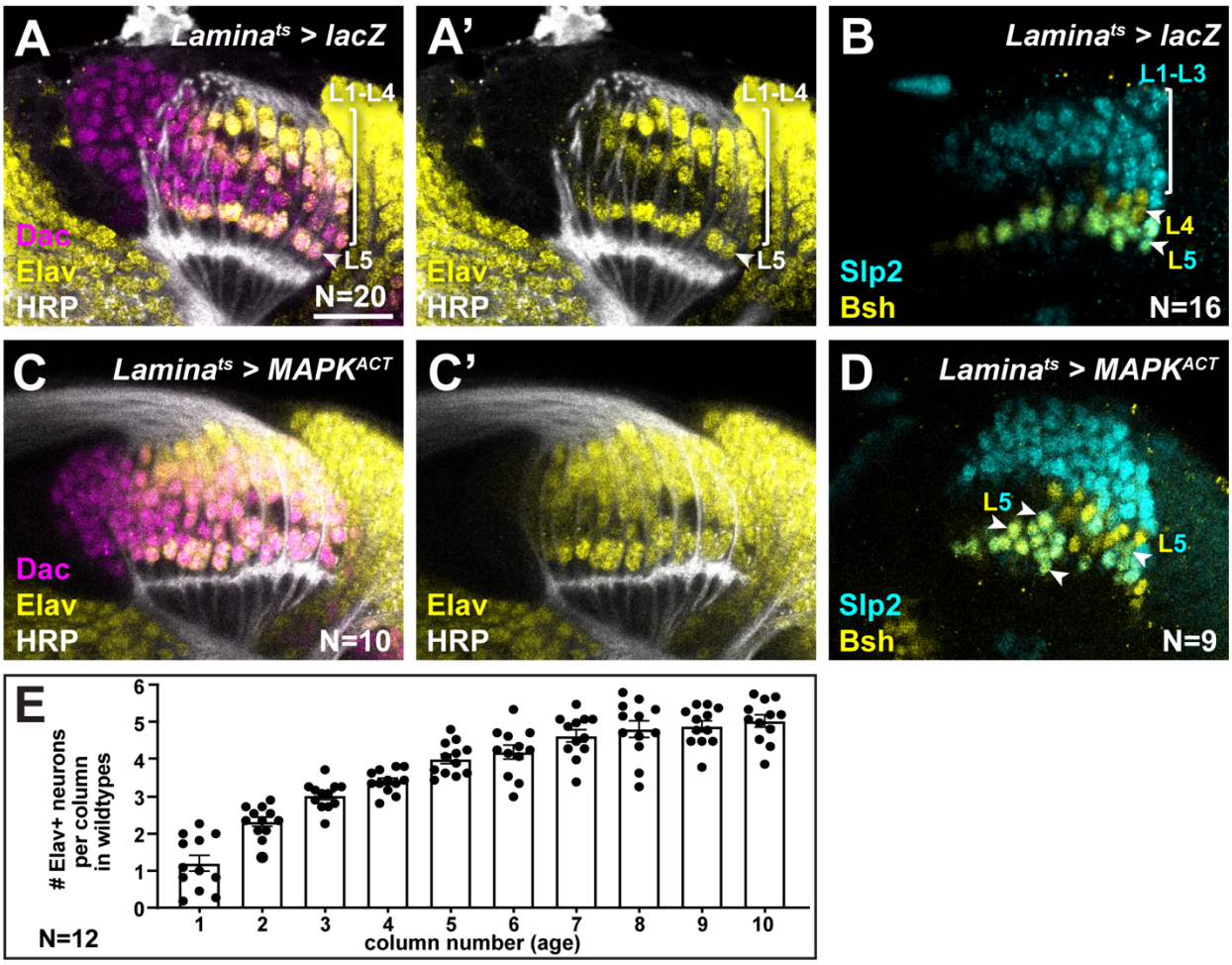
A
Lamina^ts > lacZ
L1-L4
L5
Dac
Elav
HRP
N=20
A'
L1-L4
L5
Elav
HRP
B
Lamina^ts > lacZ
L1-L3
L4
L5
Slp2
Bsh
N=16
C
Lamina^ts > MAPK^ACT
Dac
Elav
HRP
N=10
C'
Elav
HRP
D
Lamina^ts > MAPK^ACT
L5
L5
Slp2
Bsh
N=9
E
Elav+ neurons per column in wildtypes
column number (age)
N=12

2

Fig. S1: Hyperactivating MAPK in the lamina drives ectopic L5 differentiation

(A,B) Control *Lamina^{ts}>lacZ* optic lobes stained for **(A)** Dac (magenta), HRP (white) and Elav (yellow), and **(B)** and L-neuron subtype specific markers Slp2 (cyan) and Bsh (yellow). A single row of Slp2 and Bsh co-expressing cells (L5s) were present in the proximal lamina. **(C,D)** *Lamina^{ts}>MAPK^{ACT}* optic lobes stained for **(C)** Dac (magenta), HRP (white) and Elav (yellow), and **(D)** and L-neuron subtype specific markers Slp2 (cyan) and Bsh (yellow). Ectopic Slp2 and Bsh co-expressing cells (L5s) were observed (arrowheads). **(E)** Quantification of the number of Elav+ cells per lamina column as a function of column number (age) in wildtype animals. Columns were fully differentiated (5 Elav+ cells) by column 7. Scale bar = 20μm.

1 **Fig. S2**

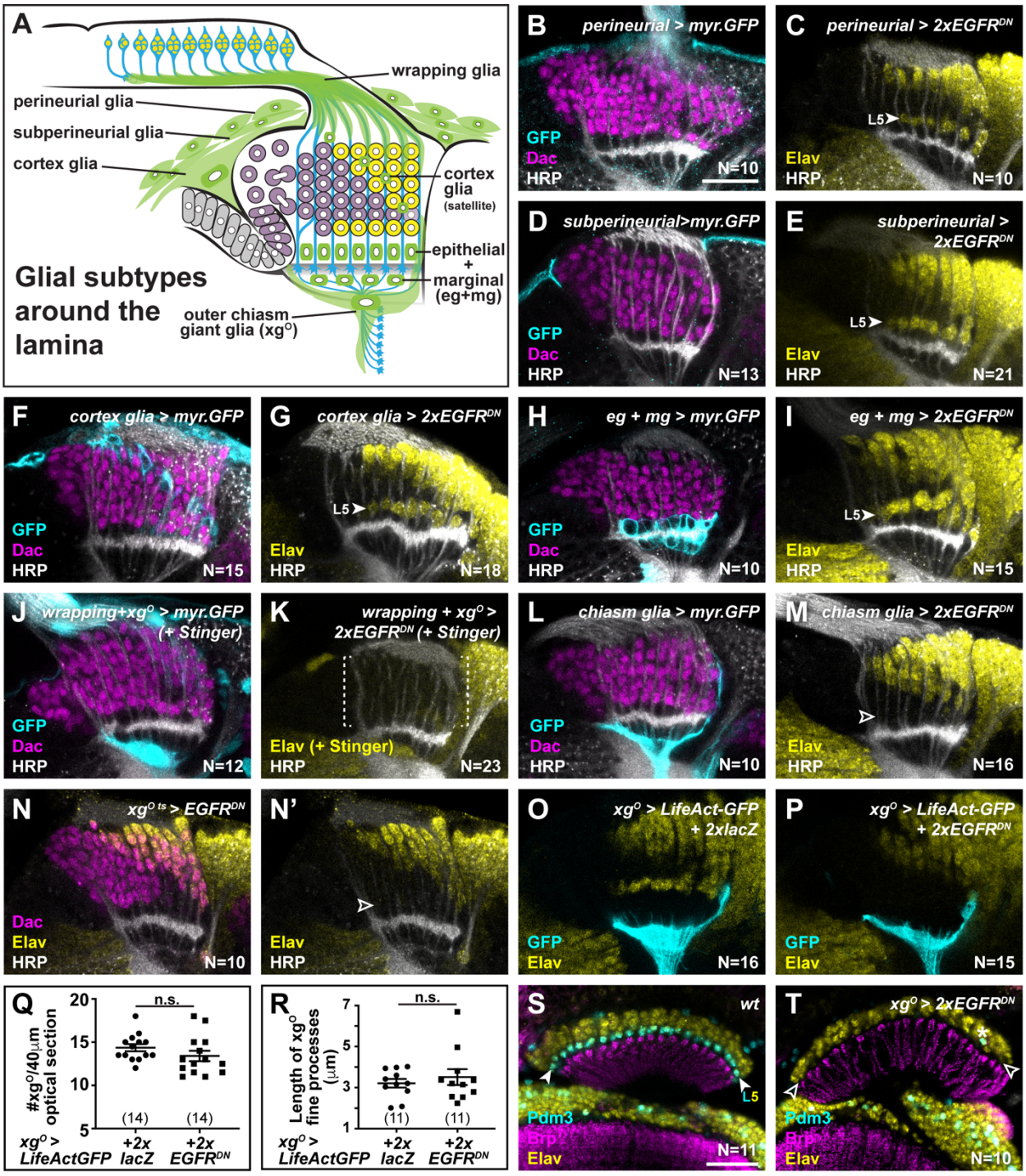
A
wrapping glia
perineurial glia
subperineurial glia
cortex glia
cortex glia (satellite)
epithelial + marginal (eg+mg)
Glial subtypes around the lamina
outer chiasm giant glia (xg^{O})
B perineurial > myr.GFP
GFP
Dac
HRP
N=10
C perineurial > 2xEGFR^{DN}
L5
Elav
HRP
N=10
D subperineurial>myr.GFP
GFP
Dac
HRP
N=13
E subperineurial > 2xEGFR^{DN}
L5
Elav
HRP
N=21
F cortex glia > myr.GFP
GFP
Dac
HRP
N=15
G cortex glia > 2xEGFR^{DN}
L5
Elav
HRP
N=18
H eg + mg > myr.GFP
GFP
Dac
HRP
N=10
I eg + mg > 2xEGFR^{DN}
L5
Elav
HRP
N=15
J wrapping+xg^{O} > myr.GFP (+ Stinger)
GFP
Dac
HRP
N=12
K wrapping + xg^{O} > 2xEGFR^{DN} (+ Stinger)
Elav (+ Stinger)
HRP
N=23
L chiasm glia > myr.GFP
GFP
Dac
HRP
N=10
M chiasm glia > 2xEGFR^{DN}
Elav
HRP
N=16
N xg$^{O\,ts}$ > EGFR^{DN}
Dac
Elav
HRP
N=10
N'
Elav
HRP
O xg^{O} > LifeAct-GFP + 2xlacZ
GFP
Elav
N=16
P xg^{O} > LifeAct-GFP + 2xEGFR^{DN}
GFP
Elav
N=15
Q
#xg^{O}/40µm optical section
20
15
10
5
n.s.
(14)
(14)
xg^{O} > LifeActGFP
+2x lacZ
+2x EGFR^{DN}
R
Length of xg^{O} fine processes (µm)
7
5
3
1
n.s.
(11)
(11)
xg^{O} > LifeActGFP
+2x lacZ
+2x EGFR^{DN}
S wt
L5
Pdm3
Brp
Elav
N=11
T xg^{O} > 2xEGFR^{DN}
Pdm3
Brp
Elav
N=10

2

Fig. S2: A Gal4 screen identifies xg^O as the glial sub-type that regulates L5 neuronal differentiation

(A) Schematic of the developing lamina and associated glial types (green; labelled). **(B)** A perineurial glia specific Gal4 drives expression of myr.GFP stained for GFP (cyan), Dac (magenta) and HRP (white). **(C)** Perineurial glia specific expression of $EGFR^{DN}$ stained for Elav (yellow) and HRP (white). L5 differentiation was not affected. **(D)** A subperineurial glia specific Gal4 drives expression of myr.GFP stained for GFP (cyan), Dac (magenta) and HRP (white). **(E)** Suberineurial glia specific expression of $EGFR^{DN}$ stained for Elav (yellow) and HRP (white). L5 differentiation was not affected. **(F)** A cortex glia specific Gal4 drives expression of myr.GFP stained for GFP (cyan), Dac (magenta) and HRP (white). **(G)** Cortex glia specific expression of $EGFR^{DN}$ stained for Elav (yellow) and HRP (white). L5 differentiation was not affected. **(H)** An epithelial and marginal glia (eg+mg) specific Gal4 drives expression of myr.GFP stained for GFP (cyan), Dac (magenta) and HRP (white). **(I)** Epithelial and marginal glia specific expression of $EGFR^{DN}$ stained for Elav (yellow) and HRP (white). L5 differentiation was not affected. **(J)** A wrapping glia and xg^O specific Gal4 drives expression of myr.GFP stained for GFP (cyan), Dac (magenta) and HRP (white). **(K)** Wrapping glia and xg^O specific expression of $EGFR^{DN}$ stained for Elav (yellow) and HRP (white). L1-L4 and L5 differentiation were disrupted as observed by the lack of Elav+ cells in the lamina. **(L)** A chiasm glia ($xg^{O\ and}\ xg^{inner)}$ specific Gal4 drives expression of myr.GFP stained for GFP (cyan), Dac (magenta) and HRP (white). **(M)** Chiasm glia specific expression of $EGFR^{DN}$ stained for Elav (yellow) and HRP (white). L1-L4 differentiation proceeded normally but L5 differentiation was disrupted as observed by the lack of Elav+ cells in the proximal lamina. **(N)** $Gal80^{ts}$-restricted Gal4 expression in xg^O, driving $EGFR^{DN}$ during lamina development (See Table S1) stained for Dac (magenta), Elav (yellow) and HRP (white). L5 neurons were dramatically reduced. **(O,P)** LifeAct-GFP expression driven in xg^O in **(O)** controls and **(P)** when $EGFR^{DN}$ is coexpressed. In both conditions, the fine processes from the xg^O are present. **(Q)** Quantification of xg^O numbers in control *xg^O>LifeAct-GFP+2xlacZ* and *xg^O>LifeAct-GFP + 2x$EGFR^{DN}$*. No significant difference was observed (P>0.05; Mann-Whitney U test. Error bars indicate SEM. Ns indicated in parentheses). **(R)** Quantification of the length of xg^O fine processes in control *xg^O>LifeAct-GFP+2xlacZ* and *xg^O>LifeAct-GFP + 2x$EGFR^{DN}$*. No significant difference was observed (P>0.05; Mann-Whitney U test. Error bars indicate SEM. Ns indicated in parentheses). **(S)**

1 Wildtype adult optic lobe stained for Pdm3 (L5 marker) [13], Bruchpilot (Brp; marks neuropils)
2 and Elav (yellow). **(T)** *xg^{O}>2xEGFR^{DN}* adult optic lobe stained for Pdm3 (L5 marker) [13],
3 Bruchpilot (Brp; marks neuropils) and Elav (yellow). Pdm3+ cells (L5s) are reduced
4 dramatically. Scale bar = 20μm.

Fig. S3

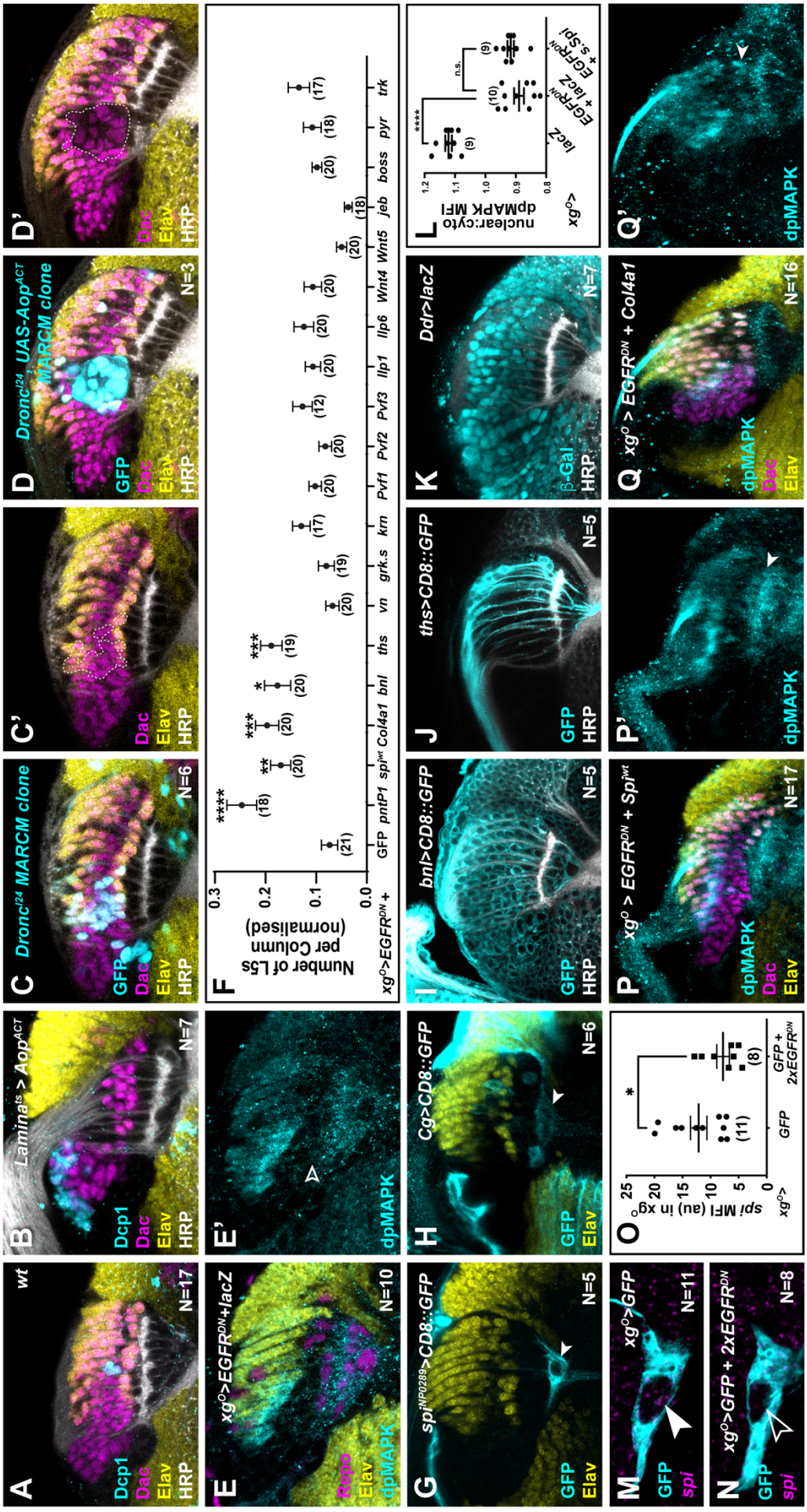
A
wt
Dcp1
Dac
Elav
HRP
N=17
B
Lamina^ts > Aop^ACT
Dcp1
Dac
Elav
HRP
N=7
C
Dronc^I24 MARCM clone
GFP
Dac
Elav
HRP
N=6
C'
Dac
Elav
HRP
D
Dronc^I24 UAS-Aop^ACT
MARCM clone
GFP
Dac
Elav
HRP
N=3
D'
Dac
Elav
HRP
E
xg^O>EGFR^DN+lacZ
Repo
Elav
dpMAPK
N=10
E'
dpMAPK
F
Number of L5s per Column (normalised)
0.3
0.2
0.1
0.0
****
**
***
*
***
(21)
(18)
(20)
(20)
(20)
(19)
xg^O>EGFR^DN +
GFP
pntP1
spi^wt
Col4a1
bnl
ths
vn
grk.s
krn
Pvf1
Pvf2
Pvf3
Ilp1
Ilp6
Wnt4
Wnt5
jeb
boss
pyr
trk
G
spi^NP0289>CD8::GFP
GFP
Elav
N=5
H
Cg>CD8::GFP
GFP
Elav
N=6
I
bnl>CD8::GFP
GFP
HRP
N=5
J
ths>CD8::GFP
GFP
HRP
N=5
K
Ddr>lacZ
β-Gal
HRP
N=7
L
nuclear:cyto dpMAPK MFI
1.2
1.1
1.0
0.9
0.8
****
n.s.
(9)
(10)
(9)
xg^O>
lacZ
EGFR^DN + lacZ
EGFR^DN + s.Spi
M
xg^O>GFP
GFP
spi
N=11
N
xg^O>GFP + 2xEGFR^DN
GFP
spi
N=8
O
spi MFI (au) in xg^O
25
20
15
10
5
0
*
(11)
(8)
xg^O>
GFP
GFP + 2xEGFR^DN
P
xg^O > EGFR^DN + Spi^wt
dpMAPK
Dac
Elav
N=17
P'
dpMAPK
Q
xg^O > EGFR^DN + Col4a1
dpMAPK
Dac
Elav
N=16
Q'
dpMAPK

Fig. S3: Multiple xg^O secreted ligands activate MAPK signalling to drive L5 neuronal differentiation

(A) A wildtype optic lobe stained for Dac (magenta), Elav (yellow), HRP (white) and Dcp-1 (cyan). **(B)** An optic lobe with lamina-specific expression of Aop^{ACT} stained for Dac (magenta), Elav (yellow), HRP (white) and Dcp-1 (cyan), showed ectopic Dcp-1 in young LPCs prior to column formation and few LPCs incorporated into each column, none of which express Elav. **(C)** Control *$Dronc^{I24}$ MARCM* clones marked by GFP stained for GFP (cyan), Dac (magenta), Elav (yellow) and HRP (white), showed a normal pattern of Elav+ cells in the lamina. **(D)** *$Dronc^{I24}$ MARCM* clones mis-expressing UAS-Aop^{ACT} marked by GFP and stained for GFP (cyan), Dac (magenta), Elav (yellow) and HRP (white). The clone, outlined by a dashed line, which included a region of the proximal lamina line was Dac+ but did not express Elav. **(E)** An optic lobe with $EGFR^{DN}$ and lacZ expressed in xg^O, stained for Elav (yellow), Repo (magenta) and dpMAPK (cyan). High levels of dpMAPK were not observed in cells in the proximal row of the lamina compared with controls (see Fig. 1G). **(F)** Quantification of the number of L5s/column normalised to control (*xg^O>GFP;* based on Elav expression) when different ligands that can activate MAPK signalling were co-expressed with $EGFR^{DN}$ in the xg^O. ($P^*<0.05$; $P^{**}<0.01$; $P^{***}<0.0005$; $P^{****}<0.0001$; Kruskal-Wallis test. Error bars indicate SEM. Ns indicated in parentheses). **(G)** *spi^{NP0289}>CD8::GFP* drove GFP (cyan) expression in xg^O (arrowhead); Elav (yellow). **(H)** *Collagen>CD8::GFP* drove GFP (cyan) expression in xg^O (arrowhead); Elav (yellow). **(I)** *bnl>CD8::GFP* showed GFP (cyan) expression in all cells in the optic lobe; HRP (white). **(J)** *ths>CD8::GFP* showed GFP (cyan) expression in photoreceptors; HRP (white). **(K)** *Ddr>lacZ* showed β-Gal (cyan) expression in the lamina; HRP (white). **(L)** Nuclear: cytoplasmic ratio of dpMAPK MFI for the genotypes indicated. ($P<0.0001$; Mann-Whitney U test. Error bars indicate SEM. Ns indicated in parentheses). **(M, N)** *spi* mRNA (magenta) detected by *in situ* hybridization chain reaction in **(M)** *xg^O>GFP* (GFP in Cyan) and **(N)** *xg^O>GFP+2x$EGFR^{DN}$*. **(O)** Quantification of *spi* MFI (arbitrary units) for (L and M). $P<0.05$; Mann-Whitney U test. Error bars indicate SEM. **(P)** Dac (magenta), Elav (yellow) and dpMAPK (cyan) when **(P)** Spi^{wt} is coexpressed with $EGFR^{DN}$ in xg^O or **(Q)** Col4a1 is coexpressed with $EGFR^{DN}$ in xg^O. Both conditions showed the presence of dpMAPK in differentiating L5 neurons (Elav+ cells in the proximal row; arrowheads). Scale bar = 20μm.

1 **Table S1: Summary of results from the glial-Gal4 screen (Fig. 2B,D, S2A-N) to identify the**
2 **glial type that regulates L5 development.**

Glial-type* > *EGFR^{DN}x2	**Elav+ cells in the proximal lamina**
Pan-glia	Absent or reduced
Perineurial glia	Present
Sub-perineurial glia	Present
Cortex glia	Present
Epithelial glia and Marginal glia (eg + mg)	Present
Wrapping glia and xg^{outer} (xg^{O})	Absent or reduced
xg^{O} +xg^{inner}	Absent or reduced
xg^{O}	Absent or reduced
xg^{Ots}	Absent or reduced

3

4 **Table S2. List of genotypes and conditions used for all experiments**
5 (Note that only female genotypes are listed though both sexes were included in our analyses)

Fig.	Panel	Genotype	Conditions
1	B	*y,w/+ ;UAS-CD8::GFP/+; hh-Gal4/repo-QF2,10xQUAS-6xm.Cherry*	Raised at 25ºC
1	C,D,G	*Canton S*	Raised at 25ºC
1	E,F	*w;;FRT80B, Dronc^{I24}*	Raised at 25ºC
1	H,I	*ey-Gal80/+; tub-Gal80^{ts}/+; R27G05/UAS-PntP1*	Raised at 18ºC till the late second larval instar (L2), then shifted to 29ºC for 48 hours
S1	A,B	*ey-Gal80/+; tub-Gal80^{ts}/+; R27G05/UAS-nls.lacZ*	Raised at 18ºC till late-L2, then shifted to 29ºC for 48 hours
S1	C,D	*ey-Gal80/+; tub-Gal80^{ts}/ UAS-rl^{sem}; R27G05/+*	Raised at 18ºC till late-L2, then shifted to 29ºC for 48 hours

S1	E	*Canton S*	Raised at 25ºC
2	A	*w^{1118}/+; tub-Gal80ts/+; Repo-Gal4/UAS-CD8::GFP*	Raised at 18ºC till late-L2, then shifted to 29ºC for 48 hours
2	B	*w^{1118}/+; tub-Gal80ts/UAS-EGFR^{DN}; Repo-Gal4/ UAS-EGFR^{DN}*	Raised at 18ºC till late-L2, then shifted to 29ºC for 48 hours
2	C	*y,w/+; UAS-CD8::GFP/+; R25A01-Gal4/+*	Raised at 29ºC
2	D	*y,w/+; UAS-CD8::GFP/ UAS-EGFR^{DN}; R25A01-Gal4/ UAS-EGFR^{DN}*	Raised at 29ºC
2	E, I	*w^{1118}/+;; R25A01-Gal4/UAS-lacZ*	Raised at 29ºC
2	F	*w^{1118}/+; UAS-EGFR^{DN}/+; R25A01-Gal4/ UAS-EGFR^{DN}*	Raised at 29ºC
2	J	*w^{1118}/+;; R25A01-Gal4/ UAS-EGFR^{DN}*	Raised at 29ºC
2	K	*y,w; GMR-Gal4/+; rho3^{PLLb}, UAS-CD8::GFP*	Raised at 29ºC
2	L	*y,w; GMR-Gal4/UAS-rho3-3xHA; rho3^{PLLb}, UAS-CD8::GFP*	Raised at 29ºC
S2	B	*y,w/+; NP6293-Gal4/+; 10xUAS-myrGFP/+*	Raised at 29ºC
S2	C	*y,w/+; NP6293-Gal4/UAS-EGFR^{DN}; UAS-EGFR^{DN}/+*	Raised at 29ºC
S2	D	*w/+; NP2276-Gal4/+; 10xUAS-myrGFP/+*	Raised at 29ºC
S2	E	*w/+; NP2276-Gal4/ UAS-EGFR^{DN}; UAS-EGFR^{DN}/+*	Raised at 29ºC
S2	F	*w^{1118}/+;; R54H02-Gal4/10xUAS-myrGFP*	Raised at 29ºC
S2	G	*w^{1118}/+; UAS-EGFR^{DN}/+; R54H02-Gal4/ UAS-EGFR^{DN}*	Raised at 29ºC
S2	H	*w^{1118}/+;; R10C12-Gal4/10xUAS-myrGFP*	Raised at 29ºC
S2	I	*$w^{1118/+}$; UAS-EGFR^{DN}/+; R10C12-Gal4/UAS-EGFR^{DN}*	Raised at 29ºC

S2	J	*w/+; Mz97-Gal4, UAS-Stinger/+; 10xUAS-myrGFP/+*	Raised at 29ºC
S2	K	*w/+; Mz97-Gal4, UAS-Stinger/UAS-EGFR^{DN}; UAS-EGFR^{DN}/+*	Raised at 29ºC
S2	L	*w^{1118}/+;; R53H12-Gal4/10xUAS-myrGFP*	Raised at 29ºC
S2	M	*w^{1118}/+; UAS-EGFR^{DN}/+; R53H12-Gal4/ UAS-EGFR^{DN}*	Raised at 29ºC
S2	N	*y,w/+; tub-Gal80^{ts}/+; R25A01-Gal4/UAS-EGFR^{DN}*	Raised at 18ºC till late-L2, then shifted to 29ºC for 48 hours
S2	O,Q	*y,w/+; UAS-LifeAct-GFP/UAS-nls.lacZ; R25A01-Gal4/UAS-nls.lacZ*	Raised at 29ºC
S2	P,R	*y,w,hsflp^{122}/+; UAS-LifeAct-GFP/UAS-EGFR^{DN}; R25A01-Gal4/UAS-EGFR^{DN}*	Raised at 29ºC
S2	S	*Canton S*	Raised at 25ºC
S2	T	*y,w/+; UAS-EGFR^{DN}/+; R25A01-Gal4/UAS-EGFR^{DN}*	Raised at 29ºC
3	A,B	*w^{1118}/+;; R25A01-Gal4/UAS-CD8::GFP*	Raised at 29ºC
3	C,D	*w^{1118}/+; UAS-EGFR^{DN}/+; R25A01-Gal4/ UAS-CD8::GFP*	Raised at 29ºC
3	E,F	*w^{1118}/+; UAS-EGFR^{DN}/+; R25A01-Gal4/ UAS-m.spi*	Raised at 29ºC
3	G,H	*w^{1118}/+; UAS-EGFR^{DN}/+; R25A01-Gal4/UAS-Cg25c::RFP*	Raised at 29ºC
3	I	*w^{1118}/+;; R25A01-Gal4/UAS-m.spi*	Raised at 29ºC
3	J	*w^{1118}/+;; R25A01-Gal4/UAS-Cg25c::RFP*	Raised at 29ºC
3	L,M	*w^{1118}/+;UAS-EGFR^{DN}/UAS-nls.lacZ; R25A01-Gal4/UAS-nls.lacZ*	Raised at 29ºC

3	N, O	*w^{1118}/+;UAS-EGFR^{DN}/ UAS-Col4a1^{EY11094}; R25A01-Gal4/UAS-m.spi*	Raised at 29ºC
S3	A	*Canton S*	Raised at 25ºC
S3	B	*ey-Gal80/+; tub-Gal80^{ts}/UAS-Aop^{ACT}; R27G05/+*	Raised at 18ºC till late-L2, then shifted to 29ºC for 48 hours
S3	C	*y,w,hsfp^{122}, Tub-Gal4, UAS-GFP/+;; FRT80B, Tub-Gal80/FRT80B, Dronc^{I24}*	Raised at 25ºC before and after heat shocking. See Mosaic analysis in Materials and Methods for more detail.
S3	D	*y,w,hsfp^{122}, Tub-Gal4, UAS-GFP/+; UAS-Aop^{ACT}/+; FRT80B, Tub-Gal80/FRT80B, Dronc^{I24}*	Raised at 25ºC before and after heat shocking. See Mosaic analysis in Materials and Methods for more detail.
S3	E	*y,w/+; UAS-EGFR^{DN}/+; R25A01-Gal4/UAS-nls.lacZ*	Raised at 29ºC
S3	F	See list of *Drosophila* stocks for specific strains used.	Raised at 29ºC
S3	G	*y,w/+; Spi^{NP0289}-Gal4/+; UAS-CD8::GFP/+*	Raised at 29ºC
S3	H	*y,w/+; Cg-Gal4/+; UAS-CD8::GFP/+*	Raised at 29ºC
S3	I	*w/+;; bnl^{NP2211}-Gal4/ UAS-CD8::GFP*	Raised at 29ºC
S3	J	*w/+; ths^{MI07139}-Gal4/+; MKRS/UAS-CD8::GFP*	Raised at 29ºC
S3	L	*w^{1118}/+; UAS-CD8::GFP/+; R25A01-Gal4/+*	Raised at 29ºC
S3	M	*y,w/+; UAS-CD8::GFP/ UAS-EGFR^{DN}; R25A01-Gal4/ UAS-EGFR^{DN}*	Raised at 29ºC
S3	O	*w^{1118}/+; UAS-EGFR^{DN}/+; R25A01-Gal4/ UAS-m.spi*	Raised at 29ºC

S3	P	*w^{1118}/+; UAS-EGFR^{DN}/+; R25A01-Gal4/UAS-Cg25c::RFP*	Raised at 29°C
S3	Q	*w^{1118}/+; Ddr^{CR01018}-Gal4/+; UAS-lacZ/+*	Raised at 29°C
4	A	*;;aos^{w11}/+*	Raised at 29°C
4	B	*w^{1118}/+;R64B07-Gal4/+;UAS-CD8::GFP/+*	Raised at 29°C
4	C	*w^{1118}; R64B07-Gal4/UAS-nls.lacZ; UAS-Dcr-2/+*	Raised at 29°C
4	C	*w^{1118}; R64B07-Gal4/UAS-aos^{RNAi}; UAS-Dcr-2/+*	Raised at 29°C

1

References

1. Luo, L., and Flanagan, J.G. (2007). Development of Continuous and Discrete Neural Maps. Neuron *56*, 284–300.
2. Hidalgo, A. (2003). The control of cell number during central nervous system development in flies and mice. *120*, 1311–1325.
3. Miguel-aliaga, I., and Thor, S. (2009). Programmed cell death in the nervous system — a programmed cell fate ? Curr. Opin. Neurobiol. *19*, 127–133.
4. Hadjieconomou, D., Timofeev, K., and Salecker, I. (2011). A step-by-step guide to visual circuit assembly in Drosophila. Curr. Opin. Neurobiol. *21*, 76–84.
5. Malin, J., and Desplan, C. (2021). Neural specification, targeting, and circuit formation during visual system assembly. Proc. Natl. Acad. Sci. *118*, e21018231182.
6. Treisman, J.E. (2013). Retinal differentiation in Drosophila. Wiley Interdiscip. Rev. Dev. Biol. *2*, 545–557.
7. Fischbach, K.F., and Dittrich, A.P.M. (1989). The optic lobe of Drosophila melanogaster. I: A. Golgi analysis of wild-type structure. Cell Tissue Res *258*, 441–475.
8. Huang, Z., and Kunes, S. (1996). Hedgehog, transmitted along retinal axons, triggers neurogenesis in the developing visual centers of the Drosophila brain. Cell *86*, 411–22.
9. Huang, Z., Kunes, S., Alcedo, J., Ayzenzon, M., Ohlen, T. Von, Noll, M., Hooper, J.E., Alexandre, C., Jacinto, A., Ingham, P.W., et al. (1998). Signals transmitted along retinal axons in Drosophila: Hedgehog signal reception and the cell circuitry of lamina cartridge assembly. Development *125*, 3753–64.
10. Sugie, A., Umetsu, D., Yasugi, T., Fischbach, K.-F., and Tabata, T. (2010). Recognition of pre- and postsynaptic neurons via nephrin/NEPH1 homologs is a basis for the formation of the Drosophila retinotopic map. Development *137*, 3303–3313.
11. Umetsu, D., Murakami, S., Sato, M., and Tabata, T. (2006). The highly ordered assembly of retinal axons and their synaptic partners is regulated by Hedgehog/Single-minded in the Drosophila visual system. Development *133*, 791–800.
12. Huang, Z., Shilo, B.Z., and Kunes, S. (1998). A retinal axon fascicle uses spitz, an EGF receptor ligand, to construct a synaptic cartridge in the brain of Drosophila. Cell *95*, 693–703.
13. Tan, L., Zhang, K.X., Pecot, M.Y., Nagarkar-Jaiswal, S., Lee, P.T., Takemura, S.Y.,

McEwen, J.M., Nern, A., Xu, S., Tadros, W., et al. (2015). Ig Superfamily Ligand and Receptor Pairs Expressed in Synaptic Partners in Drosophila. Cell *163*, 1756–1769.

14. Fernandes, V.M., Chen, Z., Rossi, A.M., Zipfel, J., and Desplan, C. (2017). Glia relay differentiation cues to coordinate neuronal development in Drosophila. Science. *357*, 886–891.

15. Apitz, H., and Salecker, I. (2014). A challenge of numbers and diversity: neurogenesis in the Drosophila optic lobe. J. Neurogenet. *28*, 1–35.

16. Freeman, M., Klämbt, C., Goodman, C.S., and Rubin, G.M. (1992). The argos gene encodes a diffusible factor that regulates cell fate decisions in the drosophila eye. Cell *69*, 963–975.

17. Akagawa, H., Hara, Y., Togane, Y., Iwabuchi, K., and Hiraoka, T. (2015). The role of the effector caspases drICE and dcp-1 for cell death and corpse clearance in the developing optic lobe in Drosophila. Dev. Biol., 1–15.

18. Fuchs, Y., and Steller, H. (2011). Programmed Cell Death in Animal Development and Disease. Cell *147*, 742–758.

19. Hasegawa, E., Kaido, M., Takayama, R., and Sato, M. (2013). Brain-specific-homeobox is required for the specification of neuronal types in the Drosophila optic lobe. Dev. Biol. *377*, 90–99.

20. Edwards, T.N., Nuschke, A.C., Nern, A., and Meinertzhagen, I. a. (2012). Organization and metamorphosis of glia in the Drosophila visual system. J. Comp. Neurol. *520*, 2067–2085.

21. Chotard, C., and Salecker, I. (2007). Glial cell development and function in the Drosophila visual system. Neuron Glia Biol. *3*, 17–25.

22. Yogev, S., Schejter, E.D., and Shilo, B.Z. (2010). Polarized secretion of drosophila EGFR ligand from photoreceptor neurons is controlled by ER localization of the ligand-processing machinery. PLoS Biol. *8*, e1000505.

23. Sopko, R., and Perrimon, N. (2013). Receptor tyrosine kinases in Drosophila development. Cold Spring Harb Perspect Biol. *5*, a009050.

24. Golembo, M., Schweitzer, R., Freeman, M., and Shilo, B. (1996). argos transcription is induced by the Drosophila EGF receptor pathway to form an inhibitory feedback loop. Development *230*, 223–230.

25. Jenett, A., Rubin, G.M., Ngo, T.-T.B., Shepherd, D., Murphy, C., Dionne, H., Pfeiffer, B.D., Cavallaro, A., Hall, D., Jeter, J., et al. (2012). A GAL4-driver line resource for Drosophila neurobiology. Cell Rep. *2*, 991–1001.
26. Viktorin, G., Riebli, N., and Reichert, H. (2013). A multipotent transit-amplifying neuroblast lineage in the central brain gives rise to optic lobe glial cells in Drosophila. Dev. Biol. *379*, 182–194.
27. Ren, Q., Awasaki, T., Wang, Y., Huang, Y., and Lee, T. (2018). Lineage-guided Notch-dependent gliogenesis by Drosophila multi-potent progenitors. Development *145*, dev160127.
28. Franzdóttir, S.R., Engelen, D., Yuva-Aydemir, Y., Schmidt, I., Aho, A., and Klämbt, C. (2009). Switch in FGF signalling initiates glial differentiation in the Drosophila eye. Nature *460*, 758–761.
29. Pinto-teixeira, F., Konstantinides, N., and Desplan, C. (2016). Programmed cell death acts at different stages of Drosophila neurodevelopment to shape the central nervous system. FEBS Lett. *590*, 2435–2453.
30. Yamaguchi, Y., and Miura, M. (2015). Review Programmed Cell Death in Neurodevelopment. Dev. Cell *32*, 478–490.
31. Davies, A.M. (2003). Regulation of neuronal survival and death by extracellular signals during development. EMBO J. *22*, 2537–2545.
32. Ballif, B.A., and Blenis, J. (2001). Molecular Mechanisms Mediating Mammalian Mitogen-activated Protein Kinase (MAPK) Kinase (MEK)-MAPK Cell Survival Signals. Cell Growth Differ. *12*, 397–408.
33. Park, H., and Poo, M.M. (2013). Neurotrophin regulation of neural circuit development and function. Nat. Rev. Neurosci. *14*, 7–23.
34. Kurada, P., and White, K. (1998). Ras Promotes Cell Survival in Drosophila by Downregulating hid Expression. *95*, 319–329.
35. Bergmann, A., Agapite, J., McCall, K., and Steller, H. (1998). The Drosophila gene hid is a direct molecular target of Ras-dependent survival signaling. Cell *95*, 331–41.
36. Bergmann, A., Tugentman, M., Shilo, B.Z., and Steller, H. (2002). Regulation of cell number by MAPK-dependent control of apoptosis: A mechanism for trophic survival signaling. Dev. Cell *2*, 159–170.

37. Zang, Y., Wan, M., Liu, M., Ke, H., Ma, S., Liu, L., and Pastor-pareja, C. (2015). Plasma membrane overgrowth causes fibrotic collagen accumulation and immune activation in Drosophila adipocytes. Elife *4*, e07187.
38. Amoyel, M., Anderson, J., Suisse, A., Glasner, J., and Bach, E.A. (2016). Socs36E Controls Niche Competition by Repressing MAPK Signaling in the Drosophila Testis. PLoS Genet. *12*, e1005815.
39. Duckhorn, J.C., Junker, I., Ding, Y., and Shirangi, T.R. (2021). Combined in situ hybridization chain reaction and immunostaining to visualize gene expression in whole-mount Drosophila central nervous. bioRxiv, 2021.08.02.454831.
40. Schindelin, J., Arganda-carreras, I., Frise, E., Kaynig, V., Longair, M., Pietzsch, T., Preibisch, S., Rueden, C., Saalfeld, S., Schmid, B., et al. (2012). Fiji : an open-source platform for biological-image analysis. Nat Methods *9*, 676–682.
41. Rebay, I., and Rubin, G.M. (1995). Yan Functions as a General Inhibitor of Differentiation and Is Negatively Regulated by Activation of the Rasl / MAPK Pathway. *81*, 857–866.
42. Asha, H., Nagy, I., Kovacs, G., Stetson, D., Ando, I., and Dearolf, C.R. (2003). Analysis of Ras-Induced Overproliferation in Drosophila Hemocytes. *215*, 203–215.
43. Gohl, D.M., Silies, M.A., Gao, X.J., Bhalerao, S., Luongo, F.J., Lin, C., Potter, C.J., and Clandinin, T.R. (2011). A versatile in vivo system for directed dissection of gene expression patterns. Nat Methods *8*, 231–237.